Weighted Differential Invariant Signatures and Applications to Shape Recognition

A DISSERTATION
SUBMITTED TO THE FACULTY OF THE GRADUATE SCHOOL
OF THE UNIVERSITY OF MINNESOTA
BY

Jessica Louise Senou

IN PARTIAL FULFILLMENT OF THE REQUIREMENTS
FOR THE DEGREE OF
DOCTOR OF PHILOSOPHY

Advisor: PETER J. OLVER

October, 2016

Acknowledgements

Firstly, I would like to express my sincere gratitude to my advisor Peter Olver for all his support throughout my arduous studies. It taught me important lessons about research, hard work and about myself, and for that alone, I thank you. Of course I'd like to thank my mother and father for pushing me in school since the beginning. Lastly, I thank my husband Setondji, for putting up with me throughout this long journey and believing in me when I didn't even believe in myself.

Dedication

To my doubtful self.

Abstract

The weighted differential invariant signature is developed to deliver more geometrical information than the signature, by combining the signature manifold with invariant measurements that capture the size of local continuous and discrete symmetries. As a consequence, the weighted signature becomes an attractive tool for the task of distinguishing between signature congruent submanifolds, which have the property that they are globally inequivalent, yet possess identical signature manifolds. Properties and relationships between such submanifolds are discussed and how these affect the weighted signature.

Contents

List of Tables

List of Figures

Chapter 1

Introduction

The task of recognizing objects under transformations and occlusions is one that the human brain solves with such unbelievable ease that at first glance it may seem almost trivial [19]. But as all of those who work in the field of computer vision know, replicating vision and interpretations of images is far more complicated. Computer vision is a relatively new field that works on programming computers to sense an environment and make decisions based on images. To this end, hundreds of methods have been employed to perform a variety of tasks such as object recognition, motion analysis, object tracking, scene reconstruction, and more. For a thorough introduction into computer vision and methodologies, as well as a plethora of references, see [69].

This thesis develops the weighted differential invariant signature and suggests its employment to the task of shape recognition under transformations. The differential invariant signature (signature), first introduced in [50] under the name classifying manifold, is parametrized by a generating set of differential invariants, thus leaving the signature manifold unchanged under the transformation, providing a means of recognizing transformed objects. For more on applications, see [2, 7, 8, 11, 12, 13, 33, 36, 45, 73]. The authors of [13] proposed the use of the planar Euclidean signature to recognize planar curves that have been translated and rotated, but theorem 2.3 in [13], was missing a hypothesis and caught the

attention of Musso and Nicolodi the authors of [49] and Mark Hickman [35], who all presented counterexamples to the incorrectly stated theorem, which obviously violated the missing hypothesis requiring the curves to be *fully regular*. This motivated the authors of [36] to start refining the signature to deal with submanifolds that were not in this category, by compromising between local and global identifying properties. The weighted signature goes significantly farther than the signature by shedding more light on local geometry.

We reformulated the computer vision problem of shape recognition in the way of Élie Cartan's Equivalence Problem which involves rewriting the problem in terms of a coframe carrying intrinsic information on the problem. The Cartan Equivalence Problem is solved via the Cartan Equivalence Method; a technique in differential geometry that indicates when a pair of geometric structures are equivalent up to a diffeomorphism [28, 41, 50, 68]. In particular, we are concerned with submanifolds equivalent under finite dimensional Lie group actions, where in the classical cases, solutions were obtain using Cartan's method of repéres mobiles [15, 16], translated into English as moving frames. As reported by Akivis [3], Cartan says he adopted his method of moving frames from Darboux who used it in his classical text, *Leçons sur la théorie générale des surfaces*, but in fact it was first introduced by Martin Bartel (1769-1836) under the name of *moving trihedrons*. Classical developments of the method of moving frame can be found in the works of Élie Cartan [15, 16], who advanced earlier contributions by Cotton, Darboux, Frenet, Serret and others into a tool for analyzing the geometric properties of submanifolds and their invariants under the action of classical transformation groups such as the Euclidean, equi-affine and projective actions on submanifolds of Euclidean space and certain homogeneous spaces. Initial efforts to place Cartan's solution methods onto firm ground were attempted in the 1970's [17, 30, 31], yet the method remained mostly confined within the classical geometric settings mentioned above. It wasn't until the late 1990's when Peter Olver investigated the consequences of the moving frame method for more general, non-geometrically based group actions. Olver's crucial breakthrough was to decouple the moving

frame theory from any reliance on frame bundles and define a moving frame as an equivariant map from the manifold being acted upon to the transformation group thereby avoiding all complications arising in the frame bundle approach.

Combining the new outlook of a moving frame as an equivariant map with the variational bicomplex [4], allowed Mark Fels and Peter Olver to place Cartan's method on firm theoretical footing while making the method broader and totally algorithmic leading to the possibility of implementation in symbolic computer packages such as MAPLE and MATHEMATICA [25, 26]. Invariantization of the variational bicomplex [44] produces the recurrence formula which completely determines the structure of the algebras of differential invariants, invariant differential forms, etc., and thus supplies us with all functional relationships or syzygies among the differential invariants from which a generating set is determined and used to parametrize the signature and solve the equivalence problem.

This thesis explores an extension of the signature to what we call weighted signatures by the addition of invariant measurements. We focus on curves and surfaces that belong to families of *signature congruent* submanifolds; globally inequivalent submanifolds with identical signatures, but the ideas extend to arbitrary dimensions and can be applied to other areas. Naturally we study characteristics of signature congruent submanifolds and how they arise to better equip the weighted signature for the task of distinguishing between family members.

The outline of this thesis is as follows. Chapter 2 introduces all of the prerequisites allowing this thesis to be self-contained. It focuses on the existence and construction of equivariant moving frames and its use in the invariantization process that ultimately leads to the signature. The latter part of chapter 2 is more relevant to the rest of the thesis since it focuses on the solution to the submanifold equivalence problem, by comparison of signatures and introduces groupoids. The main theoretical results on weighted signatures are presented in chapter 3, which naturally splits into two parts; curves and the latter on surfaces. It is here we learn that the weighted signature encodes local symmetries that are not accounted for in the regular signature. Chapter 4 contemplates the implementation of weighted

signatures in computer vision and medical imagery, and thus discusses directions of study that may prove beneficial to discrete signatures. We conclude with a summary of the main themes and findings as well as more suggestions for further work in chapter 5.

Chapter 2

Background

2.1 Equivariant Moving Frames

The method of equivariant moving frames first developed in [26], is employed to derive explicit formulas for the differential invariants, invariant forms and operators. We begin by introducing the framework needed for the existence and construction of a moving frame. Let G be an $r-$dimensional Lie group acting smoothly on an $m-$dimensional manifold M represented by the map $w : G \times M \to M$, defined on an open subset $\{e\} \times M \subset \mathcal{V} \subset G \times M$, satisfying $w(g, w(h, z)) = w(g \cdot h, z)$, and $w(e, z) = z$, for the identity element $e \in G$.

Definition 1. A *moving frame* is a smooth $G-$equivariant map $\rho : M \to G$.

There are two versions of a moving frame derived from the fact that the group can act on itself by left multiplication: $L_g(h) = g \cdot h$, or right multiplication: $R_g(h) = h \cdot g^{-1}$, producing either a left, or right moving frame. The left moving frame satisfies the equivariant condition $\rho(g \cdot z) = L_g(\rho(z)) = g \cdot \rho(z)$, while the right equivariant condition is given by $\rho(g \cdot z) = R_g(\rho(z)) = \rho(z) \cdot g^{-1}$. The right moving frame is obtained from the left by taking the inverse.

Before we continue with the moving frame existence theorem we present some needed definitions.

Definition 2. The *isotropy subgroup* of $S \subset M$ is the set $G_S = \{g \in G : g \cdot S \subset S\}$. The *global isotropy subgroup* of S is $G_S^* = \bigcap_{z \in S} G_z = \{g \in G : g \cdot z = z, \text{ for all } z \in S\}$.

Definition 3. A group acts *freely* on a manifold M if the identity element $e \in G$ is the only element that fixes a given point of the manifold. That is, $G_z = \{e\}$, for all $z \in M$. A group acts *locally freely* if G_z is discrete for all $z \in M$.

We will permit the less restrictive and more realistic locally free actions since moving frames are generally only locally defined. One way to determine if and where an action is locally free is to examine the dimension of the orbits.

Theorem 1. *An $r-$dimensional Lie group acts locally freely on a manifold if and only if the orbits are also $r-$dimensional.*

Definition 4. An action is *regular* if all the orbits have the same dimension and if for every point $z \in M$, there exist arbitrarily small neighborhoods of z that only contain connected subsets of the orbit through z.

The second condition in the regularity definition eliminates pathological actions such as the irregular flow on the torus, where a *cross-section* to the group orbits would be impossible to construct since it is only allowed to intersect an orbit once.

Definition 5. Suppose an $r-$dimensional group G acts regularly on the $m-$dimensional manifold M and has orbits of dimension s. A *(local) cross-section* K, is a submanifold of M of dimension $m - s$ that intersects each orbit transversally at a unique point.

We are now in a position to state and prove the moving frames existence theorem.

Theorem 2. *Let G act smoothly on the manifold M, then a moving frame exists in a neighborhood of $z \in M$ if and only if G acts freely and regularly near z.*

Proof. Suppose a left moving frame $\tilde{\rho} : M \to G$ exists in a neighborhood of $z \in M$. To show necessity of freeness let $g \in G_z$, so that $z = g \cdot z$. Left equivariance of the

moving frame implies that, $\tilde{\rho}(z) = \tilde{\rho}(g \cdot z) = g \cdot \tilde{\rho}(z)$. So it must be that $g = e$, implying $G_z = \{e\}$, making the action free.

Now for the necessity of regularity. Theorem 1 insures that all the orbits have the same dimension equal to r; the dimension of the group. Take a sequence of points $z_k \in M$, and a sequence of group elements $g_k \in G$, such that $z_k = g_k \cdot z$, implying that each z_k is in the orbit of z. Furthermore, assume that we have chosen the sequences in a way that $z_k \to z$ as $k \to \infty$. By continuity and left equivariance we have $\tilde{\rho}(z_k) = \tilde{\rho}(g_k \cdot z) = g_k \cdot \tilde{\rho}(z) \to \tilde{\rho}(z)$, as $k \to \infty$. Therefore $g_k \to e$ in G as $k \to \infty$ implying that the orbit through z cannot pass arbitrarily close to itself.

To prove the converse assume that the action is free and regular in a neighborhood of $z \in M$. By Frobenius' theorem [50], flat local coordinates $z = (x, y) = (x^1, \ldots, x^r, y^1, \ldots, y^{m-r}) \in G \times Y \simeq G \times \mathbb{R}^{m-r}$ can be introduced on M that locally identify M with a subset of the Cartesian product space $G \times Y$. Then the action of G on M reduces to the trivial left action of G on itself: $g \cdot z = (g \cdot x, y)$. In these coordinates a local cross-section $K \subset M$, is given by a graph $x = a(y)$. Then the map

$$\tilde{\rho}(z) = \tilde{\rho}(x, y) = x \cdot a(y),$$

is $G-$equivariant under left multiplication: $\tilde{\rho}(g \cdot z) = \tilde{\rho}(g \cdot x, y) = (g \cdot x) \cdot a(y)$, and therefore defines a left moving frame. □

Once the local existence of a moving frame is established via theorem 2, the construction of a moving frame, as the proof suggests, is related to a choice of cross-section to the $r-$dimensional orbits. Using local coordinates $z = (z_1, \ldots, z_m)$ on M, we can write the action of G on M as $w(g, z) = (w_1(g, z), \ldots, w_m(g, z)) = (g \cdot z_1, \ldots, g \cdot z_m)$. In practice one usually chooses a cross-section that will make solving the *normalization equations* as simple as possible and therefore a coordinate cross-section; $K = \{(z_1 = k_1, \ldots, z_r = k_r)\} \subset M, k_i \in \mathbb{R}$, is usually chosen leading to the normalization equations: $w_1(g, z) = k_1, \ldots, w_r(g, z) = k_r$.

Remark 1. Even though we primarily use coordinate cross-sections, other cross-sections are just as good and perhaps even better in the way of producing a larger or less restrictive subset on which the moving frame is defined, [39].

Solving the normalization equations for the r group parameters in terms of the manifold coordinates produces a right moving frame: $g = \rho(z)$. Geometrically the group element $\rho(z)$, outputted by the right moving frame is the unique group element that maps the point z to the cross-section; $\rho(z) \cdot z \in K$.

2.1.1 Prolonged Transformation Groups

Suppose $S \subset M$ is a $p-$dimensional submanifold of the $m-$dimensional manifolds, so that when G acts on M it also acts on S. Express the underlying manifold as a Cartesian product $M = X \times U$, so that for any point $z = (x, u) \in M$, we have that, $x = (x^1, \ldots, x^p) \in X \subset \mathbb{R}^p$ denoting the independent variables and $u = (u^1, \ldots, u^q) \in U \subset \mathbb{R}^{m-p}$ represents the dependent variables. Then S can be locally expressed as the graph of a function $f : X \to U$. There is an induced action on all the derivatives of f called the *prolonged transformation* defined so that it transforms the derivatives of f into the corresponding derivatives of the transformed function $g \cdot f(x)$, whose graph is the transformed submanifold $g \cdot S$. Formally, the *$n-$th prolongation of G*, denoted $G^{(n)}$, is the induced action of G on the *$n-$jet space*, $J^n(M, p) = M \times U^{(n)}$, which is coordinatized by $z^{(n)} = (x, u, u^{(n)})$, where $u^{(n)} \in U^{(n)}$ are the unordered partial derivatives of the dependent variables with respect to the independent variables up to order n. The restriction of the $n-$th jet space to the submanifold S is denoted $j_n S$. In general, the action of $G^{(n)}$ on J^n is only defined locally because it may not preserve transversality, meaning that there may be group elements that transform the submanifold in J^n into a submanifold that can no longer be expressed as the graph of a function in the given jet coordinate system. A simple example is planar lines that are graphs of functions of the form $u(x) = mx + b$. The rotation of the plane about the origin has the capability to transform any line into a vertical line which can no longer

be expressed as the graph of a function without making a coordinate change.

Higher order moving frames $\rho^{(n)} : J^n \to G^{(n)}$, are constructed in an analogous fashion as the $n = 0$ case ($J^0 = M$), as long as the existence conditions are met. Hence we need to understand the geometry of the prolonged action on jet space. In particular, we need to determine when and where the prolonged orbits achieve dimension r, at which point theorem 1 guarantees local freeness of the prolonged action and the existence of a moving frame. To this end we introduce the following definitions and theorems.

Remark 2. We will assume that our prolonged action is regular on every J^n, for $n \geq 0$.

Definition 6. The *stable orbit dimension* is the maximum prolonged orbit dimension possible. The *stabilization order* is the minimal order jet space that contains prolonged orbits of maximal dimension.

The maximum dimension of any prolonged orbit is obviously bounded by r, the dimension of the group, and in fact this orbit dimension is achieved if the group acts *locally effective on subsets* of M, meaning that the global isotropy subgroup of any open subset of M is discrete.

Theorem 3. *A Lie group acts locally effectively on subsets of a manifold if and only if the stable orbit dimension equals the dimension of the group.*

This is particularly important since the local freeness of the prolonged action is synonymous with prolonged orbits reaching dimension r the dimension of the Lie group by theorem 1.

Remark 3. The dimension of the prolonged orbit through a certain point in jet space is equal to the rank of the *Lie matrix* restricted to that point. The $n-$th order Lie matrix houses the $n-$th order prolonged infinitesimal generators of the action, [56].

Theorem 3 above guarantees that orbits of maximal dimension do exist leading to our next concern; the behavior of the prolonged orbits as we move up into higher

order jet spaces. Specifically, how do the orbit dimensions change from J^k to J^{k+1}, and is there a bound on the stabilization order? The answers to these questions are answered with the next few theorems.

Definition 7. Let s_k denote the dimension of the prolonged orbits in J^k. A group action *pseudo-stabilizes* at order k if $s_k = s_{k+1} < s_{k+2}$.

The orbit dimensions makes up a nondecreasing sequence: $s_0 \leq s_1 \leq s_2 \leq \cdots \leq r$. This coupled with the conclusion from the theorem below, that there can only be one instance of *pseudo-stabilization*, means that the stabilization order is bounded above by r, [51].

Theorem 4. *Suppose that the maximal orbit dimension of the prolonged group pseudo-stabilizes at order k. Then for any $n > k$ such that $s_n = s_{n+1}$ it must be that $s_m = s_n$ for all $m \geq n$.*

Once the maximal orbit dimension is achieved in some J^k, all higher order jet spaces continue to carry orbits of maximal dimension, [54]. This is not a global property, so at each order n, the jet space J^n can be partitioned into two subsets, $J^n = \mathcal{V}^n \cup \mathcal{S}^n$. The *regular* subset $\mathcal{V}^n$ consists of all the prolonged orbits of dimension equal to the stable orbit dimension; r. The *singular* subset $\mathcal{S}^n$, is the complement of the regular subset and thus contains all orbits of dimension less than r. Therefore $\mathcal{S}^n$ can be characterized by the linear dependence of the infinitesimal generators on J^n. We now know when and where a higher order moving frame exists.

Theorem 5. *If G acts locally effectively on subsets of M, then $G^{(n)}$ acts locally freely on $\mathcal{V}^n \subset J^n$, for n greater than or equal to the stabilization order.*

A higher order $n-$th moving frame $\rho^{(n)}$, is still constructed by solving normalization equations arising from a choice of cross-section that now lies in J^n for sufficiently large n. By denoting the acted upon manifold coordinates by $y = g \cdot x = (g \cdot x^1, \ldots, g \cdot x^p)$ and $v = g \cdot u = (g \cdot u^1, \ldots, g \cdot u^q)$, the explicit

prolonged action can be obtained by implicitly differentiating the coordinates constituting v with respect to those of y. The coordinates of the prolonged action on J^n are then written as $w^{(n)}(g, z^{(n)}) = g^{(n)} \cdot z^{(n)}$. Just as before we restrict to a coordinate cross-section by choosing to normalize r coordinates of J^n to constants: $w_1^{(n)}(g, z^{(n)}) = c_1, \ldots, w_r^{(n)}(g, z^{(n)}) = c_r$. Solving these normalization equations for the r group parameters in terms of the coordinates of J^n produces an $n-$th order right moving frame: $\rho^{(n)} : J^n \to G$.

Example 1. *The E(2) action* (2.1)*, is the* $3-$*dimensional Euclidean group acting on* $\mathbb{R}^2$ *and the planar curves within by*

$$\begin{bmatrix} y \\ v \end{bmatrix} = \begin{bmatrix} \cos\theta & -\sin\theta \\ \sin\theta & \cos\theta \end{bmatrix} \begin{bmatrix} x \\ u \end{bmatrix} + \begin{bmatrix} a \\ b \end{bmatrix}, \tag{2.1}$$

where y *and* v *are the acted upon coordinates and we assume that* $v(y)$*. By the moving frame theory we need to prolong the group action to a higher jet space in order to have any hope of producing a moving frame. Establishment of the stabilization order is achieved through inspection of the rank of the Lie matrix, that contains the prolonged infinitesimal generators of the group action. Below is* $L^{(3)}$*, the third order Lie matrix containing the prolonged infinitesimal generators on* J^3*;* $\mathbf{v_1}^{(3)}, \mathbf{v_2}^{(3)}, \mathbf{v_3}^{(3)}$ *within its columns while the rows represent the third order jet coordinates* x, u, u_x, u_{xx} *and* u_{xxx}*. For example, the third column houses the third order prolongation of the rotation generator;* $\mathbf{v_3}^{(3)} = -u\partial_x + x\partial_u + (1 + u_x^2)\partial_{u_x} + 3u_x u_{xx}\partial_{u_{xx}} + (3u_{xx}^2 + 4u_x u_{xxx})\partial_{u_{xxx}}$*.*

$$L^{(3)} = \begin{bmatrix} 1 & 0 & -u \\ 0 & 1 & x \\ 0 & 0 & 1 + u_x^2 \\ 0 & 0 & 3u_x u_{xx} \\ 0 & 0 & 3u_{xx}^2 + 4u_x u_{xxx} \end{bmatrix} \tag{2.2}$$

The Lie matrix attains maximal rank equal to three on J^1 *since* $1 + u_x^2 \neq 0$*, so*

we only need to prolong to J^1 in order to obtain a moving frame. Moreover, the regular set is the entire space; $\mathcal{V}^1 = J^1$ implying $\mathcal{V}^n = J^n$ for all $n > 0$.

The prolonged action is computed by continually applying the implicit differential operator: $D_y = \dfrac{D_x}{\cos\theta - u_x \sin\theta}$, to the dependent acted upon coordinate v. The third prolongation is given by $(x, u, u_x, u_{xx}, u_{xxx}) \mapsto (y, v, v_y, v_{yy}, v_{yyy})$ where,

$$D_y(v) = v_y = \frac{\sin\theta + u_x \cos\theta}{\cos\theta - u_x \sin\theta}, \tag{2.3}$$

$$D_y(v_y) = v_{yy} = \frac{u_{xx}}{(\cos\theta - u_x \sin\theta)^3}, \tag{2.4}$$

$$D_y(v_{yy}) = v_{yyy} = \frac{u_{xxx}(\cos\theta - u_x \sin\theta) + 3u_{xx}^2 \sin\theta}{(\cos\theta - u_x \sin\theta)^5}. \tag{2.5}$$

Now that we know a moving frame exists and we've prolonged the action to a sufficiently high jet space, we need to choose a cross-section in J^1 and solve for a first order moving frame. We choose the standard coordinate cross-section $y = v = v_y = 0$, producing the right moving frame $\rho^{(1)} : J^1 \to E(2)$, given by

$$\theta = -\tan^{-1} u_x, \quad a = -\frac{x + uu_x}{\sqrt{1 + u_x^2}}, \quad b = \frac{xu_x - u}{\sqrt{1 + u_x^2}}. \tag{2.6}$$

Example 2. *The action in equation (2.7) is derived from a subgroup of the $6-$dimensional Euclidean group $SE(3)$. It is only $4-$dimensional and involves translations in any direction but rotations only about the $u-$axis.*

$$\begin{bmatrix} X \\ Y \\ V \\ W \end{bmatrix} = \begin{bmatrix} \cos\theta & -\sin\theta & 0 & a \\ \sin\theta & \cos\theta & 0 & b \\ 0 & 0 & 1 & c \\ 0 & 0 & 0 & 1 \end{bmatrix} \begin{bmatrix} x \\ y \\ u \\ 1 \end{bmatrix}. \tag{2.7}$$

This action consists of a rotation about the $u-$axis and translation in each coordinate. We are interested in how surfaces and space curves are affected so we look for two moving frames; one on $J^n(\mathbb{R}^3, 1)$ and the other on $J^n(\mathbb{R}^3, 2)$ for sufficiently large n (n is likely to be different for the two cases).

First consider how the action affects space curves that can be locally represented by $c(x) = (x, y(x), u(x))$. *In this case, the four infinitesimal generators prolonged to* $J^2(\mathbb{R}^3, 1)$ *are represented in the columns of the second order Lie matrix below where the rows represent the jet coordinates* $x, y, u, y_x, u_x, y_{xx}$ *and* u_{xx}.

$$L^{(2)} = \begin{bmatrix} 1 & 0 & 0 & y \\ 0 & 1 & 0 & -x \\ 0 & 0 & 1 & 0 \\ 0 & 0 & 0 & -(1+y_x)^2 \\ 0 & 0 & 0 & -y_x u_x \\ 0 & 0 & 0 & -3y_x y_{xx} \\ 0 & 0 & 0 & -(2y_x u_{xx} + u_x y_{xx}) \end{bmatrix} \tag{2.8}$$

We are looking to acquire a first order moving frame defined on the entire first order jet space J^1 *since* $(1 + y_x^2) \neq 0$. *First the action is prolonged to at least* J^1 *by continually applying the implicit differential operator* $D_X = \dfrac{D_x}{\cos\theta - y_x \sin\theta}$ *to the dependent jet coordinates,* Y *and* U. *The second prolongation is explicitly given by*

$$\begin{aligned} Y_X &= \frac{\sin\theta + y_x \cos\theta}{\cos\theta - y_x \sin\theta}, \\ U_X &= \frac{u_x}{\cos\theta - y_x \sin\theta}, \\ Y_{XX} &= \frac{(\cos\theta - y_x \sin\theta)(y_{xx}\cos\theta) + (y_{xx}\sin\theta)(\sin\theta + y_x\cos\theta)}{(cos\theta - y_x \sin\theta)^3}, \\ U_{XX} &= \frac{u_{xx}(\cos\theta - y_x\sin\theta) - u_x(\cos\theta - y_x\sin\theta)}{(\cos\theta - y_x\sin\theta)^3}. \end{aligned}$$

We choose the cross-section $x = y = u = y_x = 0$ *and find that the moving frame is given by*

$$\theta = \tan^{-1}(-y_x), \quad a = -\frac{x + yy_x}{\sqrt{1+y_x^2}}, \quad b = \frac{xy_x - y}{\sqrt{1+y_x^2}}, \quad c = -u. \tag{2.9}$$

Now consider the moving frame on $J^n(\mathbb{R}^3, 2)$. In this case there are two independent variables x and y and therefore the four third order prolonged infinitesimal generators are,

$$\begin{aligned}
\mathbf{v_1}^{(3)} &= \partial_x, \\
\mathbf{v_2}^{(3)} &= \partial_y, \\
\mathbf{v_3}^{(3)} &= \partial_u, \\
\mathbf{v_4}^{(3)} &= y\partial_x - x\partial_y + u_y\partial_{u_x} - u_x\partial_{u_y} + 2u_{xy}\partial_{u_{xx}} + (u_{yy} - u_{xx})\partial_{u_{xy}} - 2u_{xy}\partial_{u_{yy}} \\
&\quad + (2u_{xyy} - u_{xxx})\partial_{u_{xxy}} + 3u_{xxy}\partial_{u_{xxx}} + (u_{yyy} - 2u_{xxy})\partial_{u_{xyy}} - 3u_{xyy}\partial_{u_{yyy}}.
\end{aligned}$$

From these vector fields, we see that the third order Lie matrix will have maximal rank on J^1 so long as u_x or u_y is nonzero. Once again we prolong the action by continually applying the implicit differential operators $D_X = \cos\theta D_x - \sin\theta D_y$ and $D_Y = \sin\theta D_x + \cos\theta D_y$ to the dependent jet coordinate U. The second order prolonged action is,

$$\begin{aligned}
U_X &= u_x\cos\theta - u_y\sin\theta, \\
U_Y &= u_y\cos\theta + u_x\sin\theta, \\
U_{XX} &= u_{xx}\cos^2\theta - 2u_{xy}\cos\theta\sin\theta + u_{yy}\sin^2\theta, \\
U_{YY} &= u_{yy}\cos^2\theta + 2u_{xy}\cos\theta\sin\theta + u_{xx}\sin^2\theta, \\
U_{XY} &= (u_{xx} - u_{yy})\sin\theta\cos\theta + u_{xy}(\cos^2\theta - \sin^2\theta).
\end{aligned}$$

We choose the coordinate cross-section to be $X = Y = U = U_X = 0$, obtaining the first order moving frame

$$\theta = \tan^{-1}\left(\frac{u_x}{u_y}\right), \quad a = \frac{yu_x - xu_y}{\sqrt{u_x^2 + u_y^2}}, \quad b = -\frac{xu_x + yu_y}{\sqrt{u_x^2 + u_y^2}}, \quad c = -u. \tag{2.10}$$

Totally Singular Submanifolds

Unfortunately, for many actions the singular subset $\mathcal{S}^n$, containing those points in J^n where a moving frame does not exist, is non-empty for all n.

Definition 8. A submanifold $S \subset M$ is called *totally singular* if $j_n S \subset \mathcal{S}^n$ for all $n = 0, 1, \ldots$.

Besides not admitting a moving frame, totally singular submanifolds are orbits that can be characterized by their symmetries.

Theorem 6. *A submanifold of $S \subset M$ is totally singular if and only if its isotropy subgroup does not act locally freely on the submanifold. That is, if the isotropy subgroup is not discrete.*

Remark 4. In the case of planar curves the singular subset is characterized by the vanishing of the Lie determinant or equivalently, when the rank of the Lie matrix is less than the dimension of the group, [54].

Example 3. *The totally singular $2-$dimensional submanifolds of the action* (2.7)*, are horizontal planes. By inspection of the prolonged infinitesimal generators on J^n, for $n > 0$, it is easy to see that the rank of the $n-$th Lie matrix will alway be less than maximal when restricted to a horizontal plane because all derivatives are zero. Moreover the isotropy subgroup is three dimensional consisting of translations and rotations.*

2.2 Invariantization

We now present the main purpose of moving frames as an invariantization tool used on differential functions, operators and forms to produce their group invariant counterparts. Essentially, the process of invariantization amounts to substituting the moving frame into the object of interest.

Definition 9. The *moving frame section*, $\sigma : J^n \to G \times J^n$ associated to the moving frame $\rho^{(n)}$, is the map $\sigma(z) = (\rho^{(n)}(z), z)$. The *invariantization* of a differential function $F : J^n \to N$ is the composition $\iota(F) = F \circ w^{(n)} \circ \sigma = F(\rho^{(n)}(z) \cdot z)$.

Geometrically, invariantization of a function $F : M \to N$ restricts the function to the chosen cross-section by pulling F back by the moving frame section while requiring that the differential invariants, $\rho^{(n)}(z)\cdot z$, be constant along the group orbits. The invariantization of something which is already invariant changes nothing and in fact invariantization defines a projection, that depends on the particular moving frame, from differential functions to differential invariants.

Definition 10. The *invariantization* of a differential form Ω on J^∞ is the invariant differential form

$$\iota(\Omega) = \sigma^*(\pi_J(w^*\Omega)).$$

In the definition above, the first step, associated with the most inner operation $w^*\Omega$, is to take group and manifold differentials of the appropriate acted upon manifold coordinates as specified by the form Ω. Then π_J projects the differential form $w^*\Omega$ to jet space by dropping all the group differentials. Finally, the differential form $\pi_J(w^*\Omega)$, is pulled back by the moving frame section, completing the process.

Theorem 7. *Let $\rho(z)$ be the moving frame solution to the normalizations equations $w_1(g,z) = c_1, \ldots, w_r(g,z) = c_r$. Then*

$$I_1(z) = w_{r+1} \circ \sigma(z), \ldots, I_{m-r}(z) = w_m \circ \sigma(z), \tag{2.11}$$

form a complete system of functionally independent invariants on M called the normalized invariants.

The theorem and terminology above can be extended to a higher order moving frame, $\rho^{(n)}$, by pulling back the jet coordinates of J^n by the moving frame section producing a complete system of functionally independent differential invariants, i.e., the *normalized invariants* of order less than or equal to n. Constructing the normalized invariants in this way, by prolonging the transformation and then substituting the moving frame, is tedious and unnecessary. The basic method due to Lie and Tresse [70], is to apply invariant differential operators $\mathcal{D}$, to lower order

invariants to produce a complete set of independent differential invariants of any order. Those operators are given by $\mathcal{D} = \sigma^*(\mathbf{D}y)^{-T} \cdot \mathbf{D}$, where $\mathbf{D}$ is the vector of implicit differential operators. Dual to the invariant differential operators are the basic invariant $1-$forms, $\omega = \sigma^*(\mathbf{D}y) \cdot d\mathbf{x}$.

Example 4. *In order to produce Euclidean differential invariants and the invariant differential operator we substitute the moving frame equation* (2.6) *into the prolonged action and the implicit differential operator respectively. The first two Euclidean differential invariants are*

$$\iota(u_{xx}) = \frac{u_{xx}}{(1+u_x^2)^{3/2}}, \qquad \iota(u_{xxx}) = \frac{(1+u_x^2)u_{xxx} - 3u_x u_{xx}^2}{(1+u_x^2)^3}, \tag{2.12}$$

and the invariant differential operator is $\mathcal{D} = \dfrac{D_x}{\sqrt{1+u_x^2}}$, *while the Euclidean arc-length form is* $ds = \sqrt{1+u_x^2}dx$. *You will notice that the lowest order differential invariant is in fact the Euclidean curvature which we will denote by* κ.

Example 5. *The explicit formulas for the generating invariants on* $J^n(\mathbb{R}^3, 1)$ *for the action* (2.7), *are obtained by substituting the moving frame* (2.9) *into the jet coordinates. For instance,*

$$\kappa = \iota(y_{xx}) = \frac{y_{xx}}{(1+y_x^2)^{3/2}}, \qquad \tau = \iota(u_x) = \frac{u_x}{\sqrt{1+y_x^2}}, \tag{2.13}$$

and all higher order differential invariants are obtained by repeatedly applying $\mathcal{D} = \dfrac{D_x}{\sqrt{1+y_x^2}}$ *to* κ *and* τ.

The first few lower order invariants on $J^n(\mathbb{R}, 2)$ *are obtained by substituting* (2.10) *into the prolonged group action yielding,*

$$\iota(u_y) = I_{01} = \sqrt{u_x^2 + u_y^2}$$
$$\iota(u_{xx}) = I_{20} = \frac{u_{xx}u_y^2 - 2u_x u_y u_{xy} + u_{yy}u_x^2}{\sqrt{u_x^2 + u_y^2}}$$
$$\iota(u_{xy}) = I_{11} = \frac{(u_{xx} - u_{yy})u_x u_y + u_{xy}(u_y^2 - u_x^2)}{u_x^2 + u_y^2}$$
$$\iota(u_{yy}) = I_{02} = \frac{u_{yy}u_y^2 + 2u_{xy}u_x u_y + u_{xx}u_x^2}{u_x^2 + u_y^2}.$$

where $I_{nm} = \iota\left(\dfrac{\partial^{n+m}u}{\partial x^n \partial y^m}\right)$.

Similarly, we obtain the invariant differential operators by invariantizing the implicit differential operators to get

$$\mathcal{D}_1 = \frac{u_y D_x - u_x D_y}{\sqrt{u_x^2 + u_y^2}}, \quad \mathcal{D}_2 = \frac{u_x D_x + u_y D_y}{\sqrt{u_x^2 + u_y^2}}.$$

The basic invariant $1-$*forms are found using the formula* $\omega = P \cdot\ dx$ *where* $\mathcal{D} = Q^T\mathbf{D} = P^{-T}\mathbf{D}$. *In our case*

$$Q = \frac{1}{\sqrt{u_x^2 + u_y^2}} \begin{bmatrix} u_y & u_x \\ -u_x & u_y \end{bmatrix},$$

so that the two basic invariant $1-$*forms are,*

$$\iota(dx) = \omega_1 = \frac{u_y}{\sqrt{u_x^2 + u_y^2}}\, dx - \frac{u_x}{\sqrt{u_x^2 + u_y^2}}\, dy, \tag{2.14}$$
$$\iota(dy) = \omega_2 = \frac{u_x}{\sqrt{u_x^2 + u_y^2}}\, dx + \frac{u_y}{\sqrt{u_x^2 + u_y^2}}\, dy. \tag{2.15}$$

The invariantization process obeys all basic algebraic laws such as associativity, distributivity and commutativity, but as we will see in the next section it does not commute with differentiation.

2.3 Recurrence Formula and Syzygies

The recurrence formula arises from the fact that the invariantization operation ι, does not commute with the exterior derivative: $d\iota(F) \neq \iota(dF)$. Moreover, the entire structure of the algebra of differential invariants including classification of *syzygies*; functional relationships among differential invariants, is obtained without knowledge of the explicit formulas for the invariants, the invariant differential operators or even the moving frame. All that is required to determine the correction term $d\iota(F) - \iota(dF)$, are the prolonged infinitesimal generators and the normalization equations.

Let $\mathfrak{g} = \{\mathbf{v}_1, \ldots, \mathbf{v}_r\}$ be a basis for the infinitesimal generators of the action of G on M. These generators are calculated by differentiating the acted upon manifold coordinates with respect to the group parameters and then evaluating the group parameters at the identity, $e \in G$. The prolonged infinitesimal generators on J^n are found using the prolongation formula for vector fields, first presented in [53]. The *recurrence formula* is

$$d\iota(\Omega) = \iota(d\Omega) + \sum_{k=1}^{r} \nu^k \wedge \iota(\mathbf{v}_k(\Omega)), \tag{2.16}$$

where Ω is usually taken to be a jet coordinate or a generic differential form. The normalized Maurer-Cartan forms ν^k, are the right invariant $1-$forms associated to the action of G on itself by right multiplication, and are naturally dual to the Lie algebra $\mathfrak{g}$. It is not necessary to compute the Maurer-Cartan forms because substitution of the normalization equations into the recurrence formula allows one to solve for them explicitly.

The recurrence formula is used to minimize the number of generating invariants needed to prescribe the signature by revealing the essential syzygies.

Definition 11. Let $I_1, \ldots, I_k$ be a set of functionally independent generating differential invariants. A *syzygy* is a functional dependency among the generating invariants and their invariant derivatives.

There are two types of syzygies: *essential syzygies* and those arising from the commutation rules among the invariant differential operators. The *commutator* formula (2.17) below, stipulates that the commutator between any two invariant differential operators be a linear combination of the invariant differential operators where the coefficients A_{ij}^k are differential invariants:

$$[\mathcal{D}_i, \mathcal{D}_j] = \sum_{i=1}^{p} A_{ij}^k \mathcal{D}_k \qquad i, j = 1, \dots, p. \tag{2.17}$$

In the case of only one independent coordinate, there is only one differential invariant operator $\mathcal{D}$, and so commutator syzygies don't exist.

The essential syzygies only depend on the differentiated invariants $\mathcal{D}_J I_\nu$ for $\mathcal{D}_J = \mathcal{D}_{j_1} \cdots \mathcal{D}_{j_k}$. In addition, equation (2.17) implies that a complete system of higher order differential invariants can be obtained from those arising from a multi-index $J = (j_1, \dots, j_k)$ that is non-decreasing $1 \le j_1 \le j_2 \le \cdots \le j_k \le p$.

Example 6. *Before we can use the Euclidean recurrence formula to determine the syzygies we need to compute the three Maurer-Cartan forms ν^1, ν^2 and ν^3 by substituting the cross-section $x = u = u_x = 0$ into* (2.16)*:*

$$\begin{aligned}
0 = d\iota(x) &= \iota(dx) + \nu^1 \iota(\mathbf{v_1}(x)) + \nu^2 \iota(\mathbf{v_2}(x)) + \nu^3 \iota(\mathbf{v_3}(x)) = \omega + \nu^1 \\
0 = d\iota(u) &= \iota(du) + \nu^1 \iota(\mathbf{v_1}(u)) + \nu^2 \iota(\mathbf{v_2}(u)) + \nu^3 \iota(\mathbf{v_3}(u)) = \nu^2 \\
0 = d\iota(u_x) &= \iota(du_x) + \nu^1 \iota(\mathbf{v_1}(u_x)) + \nu^2 \iota(\mathbf{v_2}(u_x)) + \nu^3 \iota(\mathbf{v_3}(u_x)) = \kappa\omega + \nu^3
\end{aligned}$$

Thus $\nu^1 = -\omega, \nu^2 = 0$ and $\nu^3 = -\kappa\omega$, and the E(2) recurrence formula becomes

$$d\iota(F) = \iota(dF) - \iota(\mathbf{v}_1^{(n)}(F))\omega - \kappa\iota(\mathbf{v}_3^{(n)}(F))\omega. \tag{2.18}$$

and we see that all the fundamental differential invariants on J^n for $n > 2$ are syzygies involving κ and invariant derivatives thereof. For instance, the normalized differential invariants on J^4 are $\iota(u_{xx}) = \kappa$ and $\iota(u_{xxx}) = \kappa_s, \iota(u_{xxxx}) = \kappa_{ss} + 3\kappa^3$.

Example 7. *By substituting the normalized jet coordinates; $x = y = u = u_x = 0$, into the recurrence formula we obtain the Maurer-Cartan forms: $\nu^{\mathbf{1}} = -\omega_1 = \iota(dx), \nu^{\mathbf{2}} = -\omega_2 = \iota(dy), \nu^{\mathbf{3}} = -I_{01}\omega_2$ and $\nu^{\mathbf{4}} = -\dfrac{I_{20}\omega_1 + I_{11}\omega_2}{I_{01}}$. Thus the explicit recurrence formula is*

$$d\iota(\Omega) = d_1\iota(\Omega)\omega_1 + d_2\iota(\Omega)\omega_2$$

where,

$$d_1\iota(\Omega) = \iota(D_x\Omega) - \iota\Big(\mathbf{v}_1^{(n)}(\Omega) + \frac{u_{xx}}{u_y}\mathbf{v}_4^{(n)}(\Omega)\Big),$$
$$d_2\iota(\Omega) = \iota(D_y\Omega) - \iota\Big(\mathbf{v}_2^{(n)}(\Omega) + u_y\mathbf{v}_3^{(n)}(\Omega) + \frac{u_{xy}}{u_y}\mathbf{v}_4^{(n)}(\Omega)\Big).$$

By continuing to substitute higher order derivatives of U into the recurrence formula we get the explicit recurrence relations, some of which are in table 2.1.

Ω	$d_1\iota(\Omega)$	$d_2\iota(\Omega)$
U_Y	I_{11}	I_{02}
U_{XX}	$I_{30} - 2\frac{I_{20}I_{11}}{I_{01}}$	$I_{21} - 2\frac{I_{11}^2}{I_{01}}$
U_{XY}	$I_{21} - (I_{02} - I_{20})\frac{I_{20}}{I_{01}}$	$I_{12} - (I_{02} - I_{20})\frac{I_{11}}{I_{01}}$
U_{YY}	$I_{12} + 2\frac{I_{20}I_{11}}{I_{01}}$	$I_{03} + 2\frac{I_{11}^2}{I_{01}}$
U_{XXY}	$I_{31} - \frac{I_{20}}{I_{01}}(2I_{12} - I_{30})$	$I_{22} - \frac{I_{11}}{I_{01}}(2I_{12} - I_{30})$
$\vdots$	$\vdots$	$\vdots$

Table 2.1: Recurrence relations of surface invariants to action (2.7).

2.4 Equivalence and Signatures

One of the main application of the invariants produced by the moving frame method is to aid in solving problems involving equivalencies of submanifolds under Lie group transformations. Formally two submanifolds $S, \overline{S} \subset M$, are said to be $G-$*equivalent* if $\overline{S} = g \cdot S$, for some $g \in G$. The solution to this problem is based on the functional interrelationships among the fundamental differential invariants when restricted to the submanifold. The differential invariant signature is the embodiment of these relationships being that it is parametrized by a generating set of differential invariants. To make clear the concept of a signature let $\rho^{(n)} : J^n \to G$, be an $n-$th order moving frame defined on the regular subset $\mathcal{V}^n \subset J^n$ of the $n-$th jet space. For each $k \geq n$, let $I^{(k)}$ denote the set of normalized differential invariants of order $\leq k$, and denote by $j_k S$ the restriction of J^k to the submanifold S. We call $I^{(k)}\Big|_S = I^{(k)} \circ j_k S$, the $k-$*th order restricted differential invariants* and denote this set of invariants by $J^{(k)}$.

Definition 12. The $k-$*th order signature* of the submanifold S, is the set parametrized by the $k-$th order restricted differential invariants $J^{(k)}$.

The equivalence problem is further restricted to *fully regular* $p-$dimensional submanifolds having the property that the $k-$th order signature map has constant rank; $0 \leq \text{rank } dJ^{(k)} = t_k \leq p$, for all k greater than or equal to the order of the moving frame. We call t_k the *differential invariant rank* of the $k-$th order signature which is also the dimension. In the fully regular case the differential invariant ranks strictly increase with the order of the signature until stabilization occurs at order ℓ, *the differential invariant order*:

$$t_n < t_{n+1} < t_{n+2} < \cdots < t_\ell = t_{\ell+1} = \cdots = t \leq p. \tag{2.19}$$

Now the main theorem governing the solution to the equivalence problem is presented.

Theorem 8. *Let $S_1, S_2 \subset M$, be fully regular $p-$dimensional submanifolds. Then S_1 and S_2 are locally equivalent if and only if they have the same differential invariant order ℓ and their $(\ell+1)-$st order signatures are identical.*

The $(\ell+1)-$st order signature, or the *signature*, can be parametrized by the normalized invariants of orders less than or equal $\ell+1$, but in many cases fewer invariants will suffice owing to redundancies from syzygies. Inspection of the recurrence formula (2.16), enables us to reduce the number of invariants by eliminating those that can be rewritten in terms of others from a suitable finite set of differential invariants $I_1, \dots, I_s$ to parametrize the signature of a submanifold S. We define the associated *signature map* to be

$$\chi : S \to \Sigma = \chi(S) \subset \mathbb{R}^s, \qquad \chi(z) = (I_1(z), \dots, I_s(z)). \tag{2.20}$$

Remark 5. Ordinary actions on curves living in $m-$dimensional space, there are exactly $m-1$ generating differential invariants and no syzygies. Non-ordinary actions require one more generator and a single syzygy, [56]. For actions on submanifolds of dimension greater than one the question of determining the minimal number of generating differential invariants is still open.

The signature also has a keen eye for symmetries which are just self equivalencies.

Theorem 9. *Let $S \subset M$ be a fully regular $p-$dimensional submanifold. Then the number $0 \le k \le p$, of functionally independent differential invariants on S, is equal to the codimension of its isotropy group G_S: $k = p - \dim G_S$. Furthermore, G_S acts freely on S.*

Let us explore the two extreme cases: maximal and minimal rank. Clearly, maximal rank equal to p implies there only exist discrete symmetries. The number of global symmetries is given by the *index* of the submanifold, defined to be the number of points in the submanifold that map to a generic signature point. The theorem below characterizes maximally symmetric submanifolds.

Theorem 10. *A regular $p-$dimensional submanifold S, has zero differential invariant rank if and only if its symmetry group is a $p-$dimensional subgroup $H \subseteq G$, implying that S a subset of an $H-$orbit.*

The particular orbit that S is a subset of can be determined by the values taken by signature invariants due to the following theorem.

Theorem 11. *Distinct regular rank zero orbits have distinct image points under the signature map.*

Proof. Geometrically, invariantization of some differential function F at a point $z \in S$ on the rank 0 submanifold, is the value that F takes at the unique point on the cross-section lying on the orbit through z.

□

Example 8. *Let us consider all the invariants for action* (2.7) *needed to specify the signature of a rank 2 submanifold. By inspection of the recurrence relations tabulated in table 2.1, the first order invariant I_{01} is always a fundamental invariant. Assume that the other fundamental invariant is the second order differential invariant I_{11}, so that all other invariants are (locally) functions of I_{01} and I_{11}. In particular, $I_{02} = F(I_{01}, I_{11})$ and $I_{20} = G(I_{01}, I_{11})$. By performing invariant differentiation using the recurrence formula and the chain rule on F and G we discover that the third order differential invariants I_{21} and I_{12} are solvable in terms of I_{01}, I_{11}, F, G and their first order partial derivatives $\mathcal{D}_1 F$ and $\mathcal{D}_2 G$.*

$$
\begin{aligned}
\mathcal{D}_1 F = \overbrace{I_{12} + 2\frac{G I_{11}}{I_{01}}}^{\textit{recurrence relation}} &= \overbrace{\frac{\partial F}{\partial I_{01}} I_{11} + \frac{\partial F}{\partial I_{11}}\Big(I_{21} - (F-G)\frac{G}{I_{01}}\Big)}^{\textit{chain rule}}, \\
\mathcal{D}_2 F = I_{03} + 2\frac{I_{11}^2}{I_{01}} &= \frac{\partial F}{\partial I_{01}} F + \frac{\partial F}{\partial I_{11}}\Big(I_{12} - (F-G)\frac{I_{11}}{I_{01}}\Big), \\
\mathcal{D}_1 G = I_{30} - 2\frac{G I_{11}}{I_{01}} &= \frac{\partial G}{\partial I_{01}} I_{11} + \frac{\partial G}{\partial I_{11}}\Big(I_{21} - (F-G)\frac{G}{I_{01}}\Big), \\
\mathcal{D}_2 G = I_{21} - 2\frac{I_{11}^2}{I_{01}} &= \frac{\partial G}{\partial I_{01}} F + \frac{\partial G}{\partial I_{11}}\Big(I_{12} - (F-G)\frac{I_{11}}{I_{01}}\Big).
\end{aligned}
$$

The formulas above tell us that once I_{02} and I_{20} are specified, the third order invariants, I_{03} and I_{30}, will be totally determined producing all the third order differential invariants in terms of lower order ones. Then the signature map is parametrized by four invariants of order less than three; $\chi(z) = (I_{01}, I_{11}, I_{20}, I_{02})(z)$.

Recall that all the formulas above are only locally defined. It could be that at other locations on the surface the local fundamental differential invariants are I_{01} and I_{20} so that $I_{11} = H(I_{01}, I_{20})$ and $I_{02} = F(I_{01}, I_{20})$. Going through the same steps as before yields,

$$\begin{aligned}
\mathcal{D}_1 H = I_{21} - (F - I_{20})\frac{I_{20}}{I_{01}} &= \frac{\partial H}{\partial I_{01}} H + \frac{\partial H}{\partial I_{20}}\Big(I_{30} - 2\frac{I_{20}H}{I_{01}}\Big),\\
\mathcal{D}_2 H = I_{12} - (F - I_{20})\frac{H}{I_{01}} &= \frac{\partial H}{\partial I_{01}} F - \frac{\partial H}{\partial I_{20}}\Big(I_{21} - 2\frac{H^2}{I_{01}}\Big),\\
\mathcal{D}_1 F = I_{12} + 2\frac{I_{20}H}{I_{01}} &= \frac{\partial F}{\partial I_{01}} H + \frac{\partial F}{\partial I_{20}}\Big(I_{30} - 2\frac{I_{20}H}{I_{01}}\Big),\\
\mathcal{D}_2 F = I_{03} + 2\frac{H^2}{I_{01}} &= \frac{\partial F}{\partial I_{01}} F + \frac{\partial F}{\partial I_{20}}\Big(I_{21} - 2\frac{H^2}{I_{01}}\Big).
\end{aligned}$$

The second order invariants are not a generating set because all the third order invariants cannot be derived without the specification of at least one third order invariant; any one will do, so take $I_{21} = K(I_{01}, I_{20})$. Therefore, the signature map is actually parametrized by $\chi(z) = (I_{01}, I_{11}, I_{20}, I_{02}, I_{21})(z)$.

2.5 Groupoids

The theory of symmetry, as it pertains to group actions, is not completely satisfactory due to its global nature: symmetries of a structure always involve the whole structure. On the other hand local symmetries, that appear only among certain parts of the structure itself contain more fine detailed symmetry information which is described by the theory of *groupoids*, [10, 71].

Definition 13. A group transformation $g \in G_z^{loc} \subset G$ is a *local symmetry of S based at the point $z \in S$* if there is an open neighborhood $z \in U$ such that

$g \cdot (S \cap U) = S \cap (g \cdot U)$.

The subgroup of global symmetries of S are clearly local symmetries as well; $G_S \subset G_z^{loc}$, and in fact, $G_S = \bigcap_{z \in S} G_z^{loc}$. Though the local symmetries do not form a group they form a more general object called a *groupoid*.

Definition 14. A *groupoid* over a base S is a set $\mathcal{G}$ along with an injective identity map $id : S \to \mathcal{G}$, a pair of surjective maps $s, t : \mathcal{G} \to S$ called the source and target and a multiplication operation $(\alpha, \beta) \mapsto \alpha \cdot \beta$, defined on the set $\mathcal{G} \star \mathcal{G} = \{(\alpha, \beta) : s(\alpha) = t(\beta)\}$, satisfying the following conditions when defined:

1. *Source and target products:* $s(\alpha \cdot \beta) = s(\beta)$ and $t(\alpha \cdot \beta) = t(\alpha)$.
2. *Associativity:* $\alpha \cdot (\beta \cdot \gamma) = (\alpha \cdot \beta) \cdot \gamma$.
3. *Identity:* $s(id(z)) = z = t(id(z))$, while $\alpha \cdot id(z) = \alpha$ when $z = s(\alpha)$, and $id(y) \cdot \alpha = \alpha$ when $y = t(\alpha)$.
4. *Inverses:* there is a two-sided inverse α^{-1} for each $\alpha \in \mathcal{G}$ such that $s(\alpha) = t(\alpha^{-1}), t(\alpha) = s(\alpha^{-1})$ and $\alpha^{-1} \cdot \alpha = id(s(\alpha)), \alpha \cdot \alpha^{-1} = id(t(\alpha))$.

We are particularly interested in the *action groupoid* because it allows for a formal description of local symmetries. Let G be a Lie group acting on a manifold M. The *action groupoid* is the principal bundle $\mathcal{G} = G \times M$, with source map $s(g, z) = z$ and the group action being the target map; $t(g, z) = g \cdot z$. The groupoid multiplication or better thought of as composition is only valid between pairs in the set $\mathcal{G} \star \mathcal{G} = \{(\alpha, \beta) = \big((h, g \cdot z), (g, z)\big)\big) : \text{for } h, g \in G, z \in M\}$ and is given by $(h, g \cdot z) \cdot (g, z) = (h \cdot g, z)$. The inversion map is $(g, z)^{-1} = (g^{-1}, g \cdot z)$ and there is a single identity element for each point of the manifold, namely $id(z) = (e, z)$ for identity element $e \in G$.

Definition 15. Given a Lie group G acting on a manifold M, the *symmetry groupoid* of a subset $S \subset M$ is the following set of the action groupoid:

$$\mathcal{G}_S = \{(g, z) : z \in S, g \in G_z^{loc}\}. \tag{2.21}$$

Definition 16. The *symmetry orbit* of $z \in S$ is the image of source fiber, $s^{-1}\{z\}$, under the target map: $\mathcal{O}_z = t(\mathcal{G}_z) = t \circ s^{-1}\{z\} = \{g \cdot z : g \in G_z^{loc}\}$.

One distinction between groups and groupoids is that orbits may not be connected due to the fact that G_z may consist of disjoint connected subsets of a subgroup of G. This leads us to develop a more flexible definition of the index.

Definition 17. The *index* of a regular point $z \in S$, denoted ind z, is the number of connected components of the quotient G_z^{loc}/G_z^*, where $G_z^* = \{g : g \cdot z = z\}$ is the *local isotropy subgroup* of the point z.

Just like global symmetries, G_z^{loc} is a subset of a local Lie subgroup, $\widehat{G}_z^{loc}$ of dimension $p-k$, that is refered to as the *completion* of the local symmetry set G_z^{loc}. The following theorem is the local version of theorem 9, describing the connection of the local symmetry sets of a fully regular submanifold.

Theorem 12. *If S is connected fully regular submanifold of constant rank k, then its local symmetry sets all have a common $(p-k)-$dimensional connected Lie subgroup $\widehat{G}_S \subset G$ as their completion: $\widehat{G}_z^{loc} = \widehat{G}_S$ for all $z \in S$. Moreover, S is the union of $k-$parameter family of pieces of orbits of $\widehat{G}_S$.*

Chapter 3

Theory of Invariantly Weighted Signatures

3.1 Motivation

Motivation for weighted signatures was born from the desire to discriminate submanifolds belonging to families of Euclidean *signature congruent* planar curves presented in [35, 49], having the property that all family members possess identical Euclidean signature curves, but are globally inequivalent with respect to proper Euclidean motions. These signature congruent curves were themselves motivated by an incorrectly stated theorem in [13], which stated; two smooth (C^3) curves can be mapped to each other by a proper Euclidean transformation if and only if their signature curves are identical. Comparison with theorem 8 indicates the missing hypothesis requiring the curves be fully regular, i.e., have constant differential invariant rank and thus constant dimension. To understand how this missing hypothesis is exploited to construct counterexamples, consider that the Euclidean signature map is $\chi(z) = (\kappa(z), \kappa_s(z))$, parametrized by the Euclidean curvature κ and its derivative with respect to Euclidean arc-length, κ_s. The Jacobian of χ is $d\chi = [\kappa_s, \kappa_{ss}]^T$ and its rank is zero along arcs of constant curvature. There are two types of regular submanifolds of rank 0; the $1-$parameter orbits,

circles of radius r, and lines or subsets thereof, which are mapped to the point $(1/r, 0)$ and $(0, 0)$ under χ respectively. Insertion of a subset of an appropriate orbit into a smooth curve S, at a point where κ_s in such a way that smoothness is preserved will produce another curve S' with the same signature manifold as S due to the fact that χ maps the whole inserted orbit to a single point that is already present. But S' cannot be transformed using rotations and translations to make it look identical to S, making the two curves Euclidean inequivalent. Families of Euclidean signature congruent curves can be built by varying the Euclidean length of circular arcs or line segments. In the language of groupoids this amounts to altering the symmetry groupoid of the curve, or more specifically, the size of the local symmetry sets of points lying in the orbits.

A second motivation for weighted signatures is a means to quantify information portrayed in the discrete signature obtained by discretizing the original submanifold. Viewing each discretization point as a metal bead with some mass that is dependent on its location in signature space, the weight of any subset of the signature is determined by the sample points within. Letting the number of discretization points limit to infinity naturally produces a wire or sheet (depending on the dimension) with varying density. In addition, there is flexibility in the choice of density, as is described in Definition 19.

Example 9. *The four simple closed curves a,b,c and d in figure 3.1 are taken from section 4 of [49]. All have curve e as their Euclidean signature. The blue tracing is the exact curve while the red dots represent a discrete signature obtained from the use of second order centered finite differences to approximate* κ *and* κ_s *under a uniform discretization of the parameter. Notice that near the* κ *axis around values* $.05, .5$ *and* $.95$ *the sample points become densely packed. This is due to the presence of connected subsets of circles of radius* $20, 2$ *and* 1.05 *within the curves and the number of points present is a measure of the size the circular subsets. Table 3.1 below shows how many signature points lie on the* κ *axis for the four curves in figure 3.1. Each of the four curves is parametrized by discretizing the parameter* $t \in [0, 2\pi]$ *into equal subintervals of length* $\Delta t = .02$*, resulting in a*

total of 629 sample points for each curve. Centered finite differences were used to approximate first, second and third order derivatives that were substituted into the formula for κ and κ_s to approximate the discrete signature. Table 3.1 shows how many discretization points are mapped the three key points on the $\kappa-$axis which we can think of as the weight of those signature points. In the language of groupoids, more points means a larger symmetry groupoid. Then, it is clear that the curves are inequivalent.

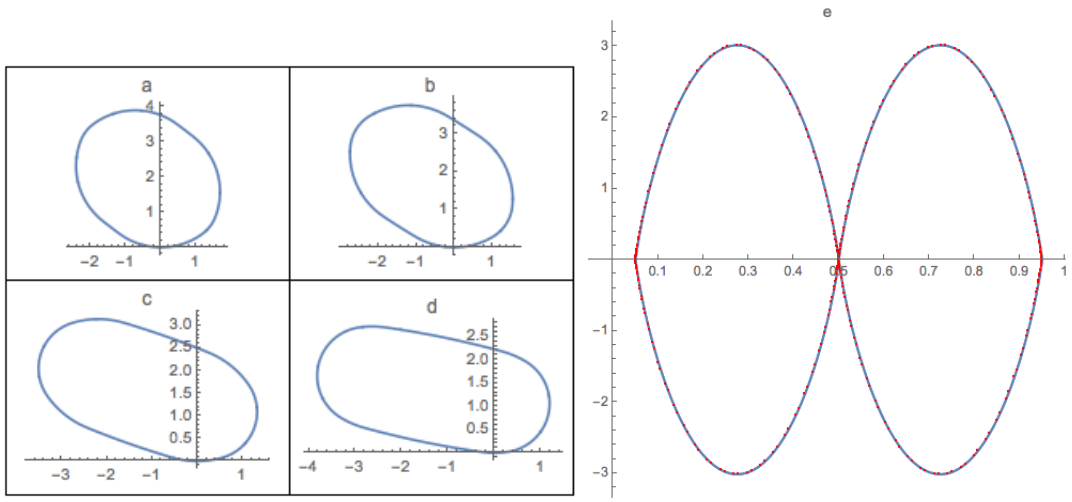

Figure 3.1: Simple closed E(2) congruent curves with common signature trace e. The actual signature is traced out in blue and the discrete signature in red.

(κ, κ_s)	a	b	c	d
(.05,0)	22	62	162	221
(.5,0)	430	350	150	30
(.95,0)	23	63	146	190

Table 3.1: Number of discretization points lying at the specified signature point for each of the four curves in figure 3.1.

3.2 Weighted Signatures

From a computer vision standpoint, the lack of distinction among signature congruent submanifolds weakens the applicability of signatures to the task of object recognition. This section introduces the main topic of this thesis; weighted signatures, which expands the range of applicability by providing more local geometrical information from measurements of invariant quantities intrinsic to the submanifold.

Definition 18. Two submanifolds are said to be *signature congruent* under the action of G, if they have the same signature trace/manifold but are $G-$inequivalent. When the signature manifold Σ is know we may refer to such submanifolds as $\Sigma-$*congruent*.

The construction of families of Euclidean signature congruent curves, by inserting subsets of regular orbit of different Euclidean arc-length, hints at a solution to our problem. Specifically, measuring intrinsic invariant quantities, such as Euclidean length, allows us to gather more geometrical information about a submanifold's local structure and symmetry.

For the purposes of the next definition, fix a particular Lie group action, so that the invariant objects referenced are all invariant with respect to this action.

Definition 19. A *weighted signature* of a smooth, $p-$dimensional submanifold S, is a pair $\mathbf{\Sigma} = (\Sigma, |\omega|)$, in which $\Sigma = \chi(S)$ is the image of S under the signature map χ and $|\omega| > 0$ is a positive, invariant $p-$density on S. The $\omega-$*weight* on $\Gamma \subset \Sigma$, denoted $\nu(\Gamma)$, is the push-forward measure via the signature map defined by

$$\nu(\Gamma) = \int_{\chi^{-1}(\Gamma)} |\omega|. \tag{3.1}$$

Remark 6. We require a positive density to avoid negative weights that introduce the possibility of cancellation resulting in calculations that provide incomplete information.

It is easy to see that two $G-$equivalent submanifolds have identical weighted signatures no matter the ω used in equation (3.1). For submanifolds of less than maximal rank the physical interpretation of the weight on $\Gamma \subset \Sigma$ in some sense, quantifies the size of the symmetry groupoid, $\mathcal{G}_{\chi^{-1}(\Gamma)}$.

3.3 Curves

We will be considering *ordinary* actions on space curves, which are those that act transitively on the underlying space and do not pseudo-stabilize. For such actions there are two generating differential invariants; the $G-$invariant curvature κ and the $G-$invariant torsion τ. Moreover, there are no syzygies among the invariant derivatives and so the signature map is $\chi(z) = (\kappa, \tau, \kappa_s, \tau_s)$ where κ_s and τ_s, are the invariant derivatives of the curvature and torsion. Locally, only one independent invariant can exist on a $1-$dimensional submanifold. Assuming this independent invariant is κ implies that $\kappa_s = f(\kappa)$ and $\tau = g(\kappa)$. Invariant differentiation of τ yields the redundant invariant $\tau_s = g'(\kappa)f(\kappa)$, [59]. Thus the signature map doesn't require τ_s, though its participation may provide some value in applications. Orbits are characterized by constant curvature and torsion and therefore are mapped to points of the form $(\kappa_0, \tau_0, 0, 0)$ under χ. Since orbits are central in the construction of signature congruent submanifolds, we would like to be able to tell when two subsets of the same orbit are globally equivalent.

Remark 7. Throughout this section we will only be considering regular orbits and ignoring totally singular orbits due to the fact that no moving frame exists on totally singular orbits and therefore the differential invariants do not exist on such orbits.

Proposition 1. *Let ω be any G invariant $1-$form on the jet space of curves embedded in $\mathbb{R}^n$. Suppose we have two sufficiently smooth, connected rank 0 curves with (non-zero) $\omega-$weighted signatures. Then the two curves are globally G equivalent modulo endpoints if and only if their $\omega-$weighted signatures are identical.*

Proof. Identical weighted signatures imply that both curves, S and S', are connected subsets of the same orbit, $\mathcal{O}$ generated by an infinitesimal generator $\mathbf{v}$ of the Lie algebra. The weight on $\chi(S)$ is given by

$$\int_S |\omega| = \int_{t_0}^{t_1} |\langle \omega; \mathbf{v} \rangle| \, dt = |\langle \omega; \mathbf{v} \rangle|(t_1 - t_0). \tag{3.2}$$

The last equality results from the fact that $\langle \omega; \mathbf{v} \rangle$ is constant along orbits. For any other connected subset $S' \subset \mathcal{O}$ with the same weighted signature as S, we get (3.2) except that the parameter t might be replaced by a change of variable $s(t) = t + a$ for $a \in \mathbb{R}$. Therefore it must be that $S' = g \cdot S$ modulo endpoints.

□

Example 10. *In section 4 of [35] a family of C^3 simply closed rectangular curves were constructed that have identical arc-length and Euclidean signature, but are rigidly inequivalent because each rectangular curve possesses different proportions. Specifically,*

$$c_\alpha(t) = \begin{cases} \textit{corner} & t \in [0, \frac{\pi}{2}] \\ \textit{line} & t \in [\frac{\pi}{2}, \frac{\pi}{2} + \alpha] \\ \textit{corner} & t \in [\frac{\pi}{2} + \alpha, \frac{3\pi}{2} + \alpha] \\ \textit{line} & t \in [\frac{3\pi}{2} + \alpha, \frac{3\pi}{2} + 10] \\ \textit{corner} & t \in [\frac{3\pi}{2} + 10, 2\pi + 10] \end{cases} \tag{3.3}$$

where $c_\alpha(t) = c_\alpha(t + 2\pi + 10)$ resulting in simple closed curves when the parameter range over the interval $[0, 2(2\pi + 10)]$. Below in figure 3.2 we provide four such curves on the left, that are traced out counterclockwise starting at the origin. The corners are drawn in black while the line segments are in green. The curve in figure 3.2e is the common signature and indicates that all the green line segments from the rectangles map to (0,0).

The Euclidean arc-length weighted signature takes $\omega = \sqrt{\dot{x}^2 + \dot{u}^2}\, dt$ in equation (3.1). The only difference among the four signature congruent curves are the proportions, it must be that $\dot{x}$ and $\dot{u}$ are the same for all four curves on the

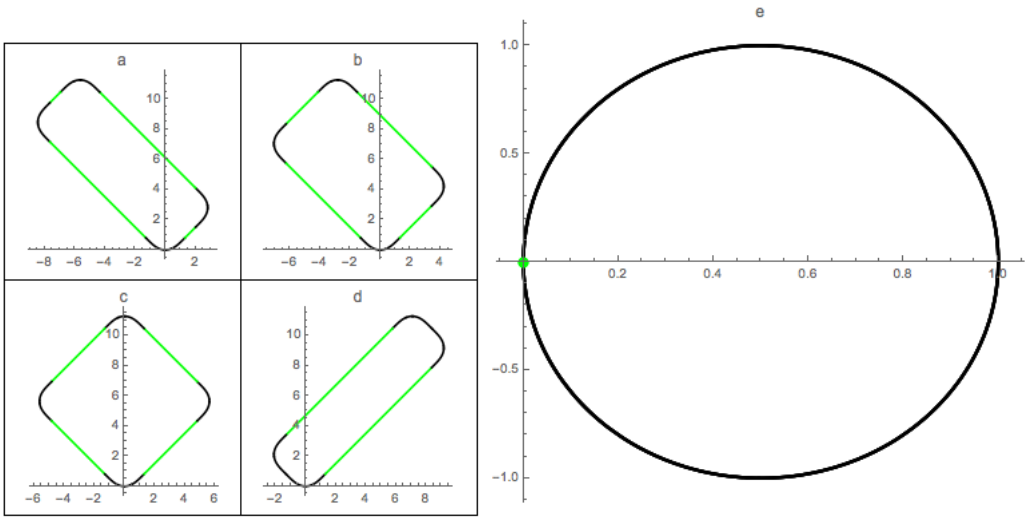

Figure 3.2: Euclidean signature congruent curves of the family described above. a. $c_1(t)$, b. $c_3(t)$, c. $c_5(t)$, d. $c_{10}(t)$, e. The common Euclidean signature plotted in the (κ, κ_s) plane. The portion of the signature outlined in black is the image of the corners of the curves which are also outlined in black while the green dot at the origin is the image of all the line segments.

respective straight line segments. Moreover, $\dot{x} = \pm\cos(\pi/4)$ *and* $\dot{u} = \pm\sin(\pi/4)$. *Then the weight of the origin* $\nu((0,0))$, *is the total length of the line segments.*

$$\nu\big((0,0)\big) = 2\int_{\frac{\pi}{2}}^{\frac{\pi}{2}+\alpha} \sqrt{\dot{x}^2+\dot{u}^2}\, dt + 2\int_{\frac{3\pi}{2}+\alpha}^{\frac{3\pi}{2}+10} \sqrt{\dot{x}^2+\dot{u}^2}\, dt \tag{3.4}$$

$$= 2\int_{\frac{\pi}{2}}^{\frac{\pi}{2}+\alpha} dt + 2\int_{\frac{3\pi}{2}+\alpha}^{\frac{3\pi}{2}+10} dt \tag{3.5}$$

$$= 2\alpha + 2(10-\alpha) \tag{3.6}$$

$$= 20. \tag{3.7}$$

Though it is obvious to us, from viewing the rectangular curves, that they are not rigidly equivalent, the current data on the total weight of $(0,0)$ *does not in any way provide information supporting this fact. Suppose we have more information and*

we know that there are 2-4 disjoint line segments within the curves and that their individual weights are given by α *or* $10 - \alpha$*. Proposition 1 implies that the line segments in the four curves are globally inequivalent and thus so are the curves.*

For the purposes of the next few results, suppose our moving frame is of *minimal order*, meaning that the projection of the moving frame cross-section, $K^n \subset J^n$ to J^k for $0 \leq k \leq n$ continues to form a cross-section to the prolonged group orbits of $G^{(k)}$ in J^k. Then there is a unique (up to constant multiple) invariant $1-$form of minimal differential order, denoted by ds, which we will call the G *arc-length form*, or just the *arc-length form* when the action is understood, [56]. Associated to ds is a natural parameter called the arc-length parameter and parametrization of a curve with respect to it is called a *unit-speed* parametrization. Under such a parametrization, all invariants are functions of the arc-length and thus invariant differentiation boils down to ordinary differentiation. The relationship between two signature congruent curve can then be formally described by theorem 13, but first we introduce some new terminology and notation. Let $c(t)$ be a parametrized space curve and let a *bivertex arc* of the curve be a connected subset whose endpoints belong to the *vertex set*; $\Lambda(c) = \{c(t_0) : \kappa'(t_0) = \tau'(t_0) = 0\}$, but whose interior points do not. Let the set of parameter values that map to the vertices be denoted by $\lambda(c) = \{t_0 : c(t_0) \in \Lambda(c)\}$.

Remark 8. To avoid pathological examples, we will restrict ourselves to curves with a finite number of connected vertices.

Theorem 13. *Let* $c_i : I_i \to \mathbb{R}^3$ *for* $i = 1, 2$*, be two unit-speed parametrized space curves smooth enough so that* $\kappa_i = \kappa \circ j_n c_i$ *and* $\tau_i = \tau \circ j_n c_i$ *are continuously differentiable and lie in the regular subset* $\mathcal{V}^n$*. Then the signature manifolds of the two curves are identical if and only if there exists a continuous piecewise* C^1 *surjection* $c : I_2 \to I_1$ *with the property that* $c'(t) = 1$ *for* $t \in I_2 \setminus c^{-1}(\lambda(c_1))$ *and it relates the signatures via* $\kappa_2 = \kappa_1 \circ c$ *and* $\tau_2 = \tau_1 \circ c$*. Moreover, the curves are globally equivalent if and only if* $c'(t) \equiv 1$*.*

Proof. Suppose that we are given two unit-speed parametrized curves with identical signatures. Then the signatures must be reparametrizations of each other, implying the existence of a continuous surjection, $c : I_2 \to I_1$, relating the two signatures via $\kappa_2 = \kappa_1 \circ c$, $\tau_2 = \tau_1 \circ c$ and $\kappa_2' = \kappa_1' \circ c$, $\tau_2' = \tau_1' \circ c$. Since $\kappa_i, \tau_i \in C^1$ and $c \in C^1$ for $t \in I_2 \setminus c^{-1}(\lambda(c_1))$, differentiation of κ_2 and τ_2 must satisfy,

$$\kappa_2' = (\kappa_1' \circ c) \cdot c' = \kappa_1' \circ c, \qquad \tau_2' = (\tau_1' \circ c) \cdot c' = \tau_1' \circ c. \tag{3.8}$$

Therefore $c'(t) = 1$, so long as κ_1' and τ_1' are non-zero, which only happens when $t \in I_2 \setminus c^{-1}(\lambda(c_1))$.

To prove the converse, let $t \in I_2 \setminus c^{-1}(\lambda(c_1))$ so that differentiation of κ_2 and τ_2 is well-defined and yields (3.8). To complete the proof, we need to show that the signatures agree at points of the form $(\kappa, \tau, \kappa', \tau') = (\kappa_0, \tau_0, 0, 0)$, for $\kappa_0, \tau_0 \in \mathbb{R}$. Let $V \subset c^{-1}(\lambda(c_1))$. If V is a singleton, continuity of c implies that $c'(V) = 1$. If V is a connected component which is not a single point, then continuity of c implies that κ_2 and τ_2 are constant on V and therefore $V \subset \lambda(c_2)$. At the endpoints of V, $\kappa_2' = \tau_2' = 0$ because $\kappa_1' = \tau_1' = 0$ at the endpoints of $c(V)$, making κ_2 and τ_2 continuously differentiable everywhere. By continuity, the signatures agree everywhere.

To prove the final statement, suppose $c'(t) \equiv 1$ so that $c(t) = t + a$ for some constant $a \in \mathbb{R}$. By theorem 8 the bivertex arcs are uniquely determined. We just have to show that corresponding vertices of c_1 and c_2 are globally equivalent. On a vertex of c_1, say $V_1 = \{c_1(t) : t \in A_1 \subset \lambda(c_1)\} \subset \Lambda(c_1)$, the generating invariants are constant while all higher order invariants are zero; $\kappa_1|_{V_1} = \kappa_0, \tau_1|_{V_1} = \tau_0$ and $\kappa_1'|_{V_1} = \tau_1'|_{V_1} = 0$. The relationship between $\chi(c_1)$ and $\chi(c_2)$ indicates that while $t \in A_1, \kappa_2 = \kappa_1 \circ c = \kappa_0, \tau_2 = \tau_1 \circ c = \tau_0$ and $\kappa_2' = \tau_2' = 0$. Thus $c^{-1}(A_1) = A_2 \subset \lambda(c_2)$ so that the $ds-$weighted signature of V_1 and $V_2 = \{c_2(t) : t \in A_2\} \subset \Lambda(c_2)$ are identical implying global equivalence by proposition 1.

□

The corollary below says that for a given signature manifold Σ, there is a unique curve with signature trace Σ that has a discrete vertex set.

Corollary 1. *Two space curves with discrete vertex sets can be mapped to each other by a G transformation if and only if their signatures are identical.*

Proof. It is obvious that the signatures are identical given that $c_2 = g \cdot c_1$, so let us consider the converse. By theorem 13, identical signatures implies that $\kappa_2 = \kappa_1 \circ c$ and $\tau_2 = \tau_1 \circ c$, where $c'(t) = 1$ for $t \in I_2 \setminus c^{-1}(\lambda(c_1))$. Non-degeneracy means that $\lambda(c_1)$ and $\lambda(c_2)$ are discrete, so by continuity of c we have that $c' \equiv 1$ and thus c_1 and c_2 are globally equivalent.

□

Unit-speed parametrizations are often inconvenient, so we turn our attention to a reformulation of the method used in [36] to distinguish between two signature congruent curves, but instead of focusing solely on *bivertex arcs*, we focus on vertices and their weights as well, allowing us to drop the assumption that there exists a minimal order moving frame.

Suppose c_1 and c_2 are signature congruent curves and let us redefine $\Lambda(c_i)$ to be the non-isolated vertices and $\mathcal{B}(c_i)$ the bivertex arcs of curve c_i (point vertices are still present as the endpoints of bivertex arcs). The structure of curve c_i is demonstrated by an ordered set called the *ordered bivertex arc decomposition (OBD)* which takes the form $\{\dots, B^i_j, V^i_{j+1}, \dots\}$ describing how the curve is assembled. This labeling is especially useful when studying simply closed curves where different labels are likely to arise from different starting point choices. For example, look back at figure 3.2 containing four Euclidean signature congruent rectangular shaped curves. The ordered bivertex decomposition for curves a, b and c, have decompositions of the form, $\{B_0, V_1, B_2, B_3, V_4, B_5, B_6, V_7, B_8, B_9, V_{10}, B_{11}\}$, starting on B_0, the bivertex arc intersecting the origin, and moving counterclockwise. The isolated vertex connecting two bivertex arcs, in this case the "corner point" of the rectangle, is mapped to (1,0) under χ. On the other hand the curve in d has the decomposition $\{B_0, V_1, B_2, B_3, B_4, B_5, V_6, B_7, B_8, B_9\}$. In this case, we obtain two more isolated vertices that are mapped to the origin under χ.

Remark 9. There are a few geometries where for certain curves there is a lower

bound on the number of bivertex arcs present. Specifically there is the four vertex theorem and the six vertex theorem. The four vertex theorem states that the planar Euclidean curvature restricted to a simple, closed, smooth plane curve has at least four local extrema, implying that $m_i \geq 4$. In the planar equiaffine case, the equiaffine curvature of a convex closed curve has at least six critical points; $m_i \geq 6$. There are no results to this effect for general group actions, [66].

Proposition 2. *Two non-singular (similarly) oriented signature congruent curves c_1 and c_2 are globally equivalent if and only if they have the same number of vertices and bivertex arcs and if there is a cyclic reordering of the ordered bivertex arc decomposition such that corresponding vertices and bivertex arcs are mapped to the identical signature manifold and have identical weights. In other words, the curves are globally equivalent if and only if the following are satisfied.*

1. *Both curves contain the same number of vertices and bivertex arcs: $n_1 = n_2 = n$ and $m_1 = m_2 = m$.*
2. *For each j, $\chi(V_j^1) = \chi(V^2_{(j+k)Mod\ (n+m)})$ and $\nu(\chi(V_j^1)) = \nu(\chi(V^2_{(j+k)Mod\ (n+m)}))$.*
3. *For each j, $\chi(B_j^1) = \chi(B^2_{(j+k)Mod\ (n+m)})$.*

where k is the same fixed integer in items 2 and 3.

Proof. It is obvious that two globally equivalent curves will satisfy the three items above so consider a pair of $\Sigma-$congruent curves c_1 and c_2, for the action of G on $\mathbb{R}^3$. We will show that there is a common $g \in G$ such that $c_2 = g \cdot c_1$.

Items two and three above require the labeling of the ordered bivertex decompositions of c_1 and c_2 coincide indicating the two curves are assembled in the same order under the same orientation using the same bivertex arcs. Without loss of generality we assume that $k = 0$ in the hypothesis so that we may write, $B_j^2 = g_j \cdot B_j^1$ for each of the m bivertex arcs and some $g_j \in G$.

Now consider the points that lie between each bivertex arc. The signature map sends these points to the $\kappa\tau-$plane. When there is an isolated point shared

by B_j^k and B_{j+1}^k, continuity of Σ implies that $B_j^2 = g \cdot B_j^1$ and $B_{j+1}^2 = g \cdot B_{j+1}^1$, for the same $g \in G$. When there is a regular connected vertex joining two bivertex arcs producing an OBD of the form, $\{\dots, B_j^k, V_{j+1}^k, B_{j+2}^k, \dots\}$, the signature point $\chi(V_{j+1}^k)$ is predetermined by continuity and lies on the $\kappa\tau-$plane specifying the orbit $\mathcal{O}$ for which $V_{j+1}^k \subset \mathcal{O}$ by theorem 11. By proposition 1, the weight $\nu(\chi(V_{j+1}^k))$ determines the exact subset, i.e. the size of the subset implying the global equivalence of the two vertices; $V_{j+1}^2 = g_{j+1} V_{j+1}^1$. Since the endpoints of these three pieces $\{\dots, B_j^k, V_{j+1}^k, B_{j+2}^k, \dots\}$ are shared it must be that $g_{j+1} = g$ as above and thus $c_2 = g \cdot c_1$.

□

Example 11. *The authors of [49] created what they call cogwheels, which are simple closed rank 1 planar curves having identical Euclidean signatures due to the fact that the curves are composed of the same distinct n "cogs". Moreover, the weighted signatures will also be identical if the same number of each of the cogs is used in the construction.*

We consider two Euclidean congruent cogwheels made using three distinct cogs, illustrated in the figure below. The three distinct cogs are outline in red, blue and green. The only significant difference between the two curves is the ordered bivertex decomposition which are not rotationally related.

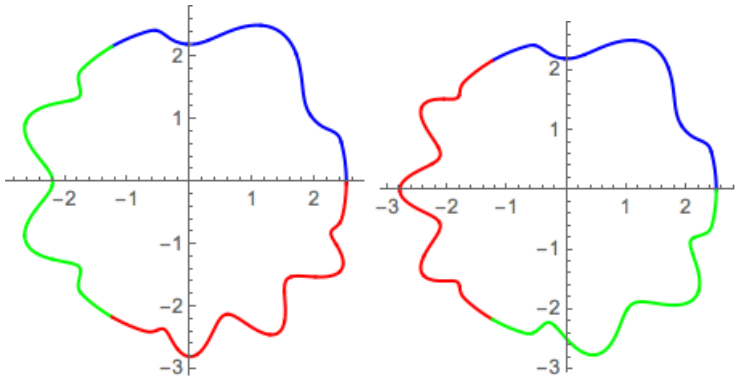

Figure 3.3: Globally inequivalent cogwheels, composed of the same three cogs outlined in red, blue and green.

3.4 Surfaces

In this section we consider Lie groups acting on $\mathbb{R}^3$ and the induced action on smooth compact surfaces that are graphs of functions of the form $u(x, y)$. Locally, there can only be two independent invariants defined on a surface resulting in three rank cases; maximally symmetric surfaces having rank 0; minimally symmetric surfaces having rank 2; and the intermediate case.

The rank 0 case for 2−dimensional submanifolds is analogous to the rank 0 case for 1−dimensional submanifolds. Specifically, theorem 10 says that such a surface is a subset of a regular 2−parameter orbit and according to theorem 9, all invariants are constant, resulting in a single point constituting the signature, which describes the orbit by theorem 11. The signature congruent submanifolds, S and S' differ in size and/or shape. The size of the symmetry groupoid of the interior, $\mathcal{G}_{\mathring{S}}$ provides information about size, while the signature of the boundary characterizes the shape. In the case that this isn't enough, the size of local symmetries can be characterized by the symmetry groupoid for points and connected segments of the boundary. Recall, the weight in some sense measures the size of symmetry groupoids. Equation (3.1) gives the weight for some subset $\Gamma \subset \chi(S) = \Sigma$ of the signature for any non-zero invariant 2−form Ω. Moreover, a general invariant 2−form takes the form $I \cdot \Omega$ for $\Omega = \iota(dx \wedge dy)$, for any differential invariant I, implying different weighted signatures of the same surface differ by a constant multiple.

Example 12. *The regular rank 0 surfaces of the action* (2.7) *are non-horizontal planes. Let us examine two signature congruent planes of the form* $u(x, y) = \alpha x + \beta y$. *Let the plane* P_1 *be the subset of the plane lying over the circular region* $D_1 = \{(x, y) : 0 \leq x^2 + y^2 \leq r^2\}$, *and let the second plane* P_2 *be the plane lying over the rectangular region* $D_2 = \{(x, y) : 0 \leq x \leq r^2, 0 \leq y \leq \pi\}$. *The image of any subset of the plane under the signature map is the single point* $\chi(u(x, y)) = (\sqrt{\alpha^2 + \beta^2}, 0, 0, 0, 0)$. *The basic invariant* 2−*form is the area form* $\Omega = dx \wedge dy$. *Thus the* Ω−*weighted signature of both submanifolds* P_1 *and* P_2 *is*

πr^2, the area of their domains D_1 and D_2. Thus, proposition 1 doesn't generalize to higher dimensional submanifolds.

The rank 2 case is analogous to the rank 1 case for 1−dimensional submanifolds in that the signature uniquely determines the submanifold since the signature invariants determine a system of ordinary differential equations by Frobenius' theorem [50]. Such surfaces only exhibit discrete symmetries resulting in parts of the signature being retraced implying that the signature wraps around to intersect itself. One obvious example of this are signature congruent surfaces arising from periodic functions, see example 13.

Example 13. *Consider the pair of signature congruent rank 2 surfaces S and S' under action* (2.7)*, that are subsets of the graph of the periodic function, $u(x, y) = \sin x + \sin y$. Let $S = \{(x, y, u(x, y)) : 0 < x, y < 2\pi\}$ and $S' = \{(x, y, u(x, y)) : 0 \leq x^2 + y^2 \leq (2\pi)^2\}$. It is easy to see from the periodicity of sine that S has trivial symmetry groupoid and that $\chi(\overline{S}) = \chi(S')$. Since $\overline{S} \neq S'$, any weighted signature will have that $\nu(\chi(S)) < \nu(\chi(S'))$, implying that these surfaces are not equivalent.*

The intermediate case is the most interesting. By theorem 9, rank 1 surfaces possess a 1−dimensional isotropy subgroup generated by the vector field $\mathbf{v}$ spanning a 1−dimensional sub-algebra to the Lie algebra. As a result, the surface is foliated by 1−parameter orbits induced by $\mathbf{v}$, which we refer to as *ruling orbits*. Each point of the 1−dimensional signature $p \in \Sigma$, is the image of a disjoint set of ruling orbits and therefore, inherits a weight associated to the total size of those ruling orbits given by

$$\nu(p) = \int_{\chi^{-1}(p)} |\omega|, \tag{3.9}$$

for any G−invariant 1−form ω. On the other hand, a connected portion $\Gamma \subset \Sigma$ is weighted by

$$\nu(\Gamma) = \int_{\chi^{-1}(\Gamma)} |\Omega|, \tag{3.10}$$

for any $G-$invariant 2$-$form Ω. The *general $G-$invariant coarea formula* in [62] provides an elegant connection between these two weights. We formalize this notion by first introducing the concept of a normal curve to the ruling orbits.

Definition 20. Under a given rank 1 surface S and a given invariant 1$-$form ω and 2$-$form Ω, a curve $C \subset S \subset \mathbb{R}^3$ will be deemed a *normal cross-section* provided it forms a cross-section to the ruling orbits that are generated by the Lie algebra member $\mathbf{v} \neq 0$ and at each point $z \in C$, we have that

$$\langle \Omega; \mathbf{v} \wedge \mathbf{w} \rangle = \langle \omega; \mathbf{v} \rangle \langle \omega; \mathbf{w} \rangle \qquad \text{for all } \ \mathbf{w} \in TC\big|_z. \tag{3.11}$$

Remark 10. The normality condition defined an underdetermined system of ordinary differential equations whose solution prescribes the tangent vector to C and as such C is not uniquely determined.

Theorem 14. *Let $C \subset S$ be a normal cross-section in the rank 1 surface S. Then*

$$\iint_S |\Omega| = \int_C \ell(\mathcal{O}_z \cap S)|\omega|, \quad \textit{where } \ \ell(\mathcal{O}_z \cap S) = \int_{\mathcal{O}_z \cap S} |\omega|. \tag{3.12}$$

Remark 11. Let S be a surface only able to be foliated by one type of 1$-$parameter orbit. If the ruling orbits are regular with continuously changing local symmetry sets then the intersection of these sets is discrete and equal to the isotropy subgroup of the entire surface implying that such surfaces are rank 2. There do exist surfaces ruled by totally singular orbits that do admit a signature or rank 1 and 2 since the surfaces doesn't necessarily adopt an isotropy subgroup that doesn't act freely on it.

Example 14. *In this example we investigate the consequences of equation* (3.11) *in the case of action* (2.7)*, which has basic invariant forms, $dx \wedge dy$ and $ds = \sqrt{1+y_x^2}\,dx$. Below in table 3.2 we have complied some of the results.*

Let $\mathbf{v} = \xi\partial_x + \eta\partial_y + \zeta\partial_u$ be the tangent vector field to some generic 1$-$parameter orbit and let $\mathbf{w} = a\partial_x + b\partial_y + c\partial_u$ be the tangent vector to a normal cross-section

Ω	ω	$\lvert\langle\Omega;\mathbf{v}\wedge\mathbf{w}\rangle\rvert = \lvert\langle\omega,\mathbf{v}\rangle\rvert\lvert\langle\omega,\mathbf{w}\rangle\rvert$
$dx\wedge dy$	ds	$(\mathbf{v}\times\mathbf{w})\cdot\mathbf{k} = \lvert\lvert\mathbf{v}\times\mathbf{k}\rvert\rvert\lvert\lvert\mathbf{w}\times\mathbf{k}\rvert\rvert$
$I_{01}\ dx\wedge dy$	ds	$\lVert(\mathbf{v}\times\mathbf{w})\times\mathbf{k}\rVert = \lVert\mathbf{v}\times\mathbf{k}\rVert\lVert\mathbf{w}\times\mathbf{k}\rVert$
$\sqrt{I_{01}^2+1}\ dx\wedge dy$	ds	$\lvert\lvert\mathbf{v}\times\mathbf{w}\rvert\rvert = \lvert\lvert\mathbf{v}\times\mathbf{k}\rvert\rvert\lvert\lvert\mathbf{w}\times\mathbf{k}\rvert\rvert$
$dx\wedge dy$	$\tau\ ds$	$(\mathbf{v}\times\mathbf{w})\cdot\mathbf{k} = (\mathbf{v}\cdot\mathbf{k})(\mathbf{w}\cdot\mathbf{k})$
$I_{01}\ dx\wedge dy$	$\tau\ ds$	$\lVert(\mathbf{v}\times\mathbf{w})\times\mathbf{k}\rVert = (\mathbf{v}\cdot\mathbf{k})(\mathbf{w}\cdot\mathbf{k})$
$\sqrt{I_{01}^2+1}\ dx\wedge dy$	$\tau\ ds$	$\lvert\lvert\mathbf{v}\times\mathbf{w}\rvert\rvert = (\mathbf{v}\cdot\mathbf{k})(\mathbf{w}\cdot\mathbf{k})$

Table 3.2: Results of equation (3.11) restricted to invariant forms under action (2.7).

C, in a surface ruled by those generic orbits. We illustrate how we obtained the result in the first row of table 3.2. On the orbit we have that $y_x = \dfrac{y_t}{x_t} = \dfrac{\eta}{\xi}$ *and* $\dfrac{dx}{dt}dt = dx = \xi\ dt$. *Similarly on the normal cross-section C,* $y_x = \dfrac{y_{\mathfrak{t}}}{x_{\mathfrak{t}}} = \dfrac{b}{a}$ *and* $dx = a\ d\mathfrak{t}$. *Then the two terms on the right hand side of equation* (3.11) *become,*

$$|\langle\omega;\mathbf{v}\rangle| = \sqrt{1+(\eta/\xi)^2}|\xi| = \sqrt{\xi^2+\eta^2}, \qquad |\langle\omega;\mathbf{w}\rangle| = \sqrt{1+(b/a)^2}|a| = \sqrt{a^2+b^2}.$$

In order to compute the left hand side we need the wedge product between the two tangent vectors; $\mathbf{v}\wedge\mathbf{w} = (\xi b-\eta a)\ dx\wedge dy + (\xi c-\zeta a)\ dx\wedge du + (\eta c-\zeta b)\ dy\wedge du$. *Then since the* $2-$*form* $\Omega = dx\wedge dy$ *we need only take the first term of the wedge product so,* $|\langle\Omega;\mathbf{v}\wedge\mathbf{w}\rangle| = b\xi - a\eta$. *Therefore the tangent vector field* $\mathbf{w}$ *is required to satisfy,* $b\xi - a\eta = \sqrt{(a\xi)^2+(a\eta)^2+(b\xi)^2+(b\eta)^2}$, *which can be rewritten as,* $(\mathbf{v}\times\mathbf{w})\cdot\mathbf{k} = ||\mathbf{v}\times\mathbf{k}||||\mathbf{w}\times\mathbf{k}||$. *The left hand side can be interpreted as the volume of the parallelepiped spanned by the three vectors, while the right hand side is the product of the length of the horizontal projections of* $\mathbf{v}$ *and* $\mathbf{w}$. *This makes perfect sense because the altitude of the parallelepiped is the length of* $\mathbf{k}$ *which is one.*

Now let us compute the formula given in the last row of table 3.2, by taking $\Omega = \sqrt{1+I_{01}^2}\ dx\wedge dy$, *which is the basic invariant* $2-$*form or the surface area element for the full Euclidean action SE(3), and* $\omega = \tau\ ds = u_x\ dx$. *On the orbit* $u_x = \dfrac{\zeta}{\xi}$ *and* $dx = \xi\ dt$ *while on the normal cross-section* $u_x = \dfrac{c}{a}$ *and* $dx = a\ d\mathfrak{t}$.

Then $|\langle\omega;\mathbf{v}\rangle||\langle\omega;\mathbf{w}\rangle| = c\zeta$. *On the other hand, if the parametrized curve* $z(t) = (x(t), y(t), u(t))$ *is on the surface defined by* $u(x, y)$, *then* $u(t) = u(x(t), y(t))$ *and differentiation with respect to the parameter yields,* $u_t = u_x x_t + u_y y_t$. *If* $z(t)$ *parametrizes an orbit then,* $\zeta = \xi u_x + \eta u_y$ *and in the case of the normal cross-section we get,* $c = au_x + bu_y$. *Solving for* u_x *and* u_y *using these two equations produces*

$$u_x = \frac{\eta c - \zeta b}{\eta a - \xi b}, \qquad u_y = \frac{\zeta a - \xi c}{\eta a - \xi b}.$$

Substitution of the above equations into $\sqrt{1 + I_{01}^2}$ *and replacing* $|dx \wedge dy|$ *with* $\xi b - \eta a$ *gives us the left hand side of equation* (3.11),

$$\sqrt{(\eta b - \xi b)^2 + (\zeta a - \xi c)^2 + (\eta c - \zeta b)^2}\,\left|\frac{\xi\ b - \eta\ a}{\eta a - \xi b}\right| = ||\mathbf{v} \times \mathbf{w}||.$$

Since we are assuming that the surface is locally the graph of a function $u(x, y)$, *the orbits project to distinct curves in the* $xy-$*plane so we need only integrate over regions in this plane when using the* $G-$*invariant coarea formula* (3.12). *Hence we need only be concerned with the horizontal projection of* $\mathbf{w}$.

Lastly, we use the $G-$*invariant coarea formula* (3.12) *to compute the weight of a rank 1 surface and its ruling orbits. Let* $S_1 = \{(x, y, x^2 + y^2 : for\ 0 \leq x^2 + y^2 \leq 1\}$ *and* $S_2 = \{(x, y, x^2 + y^2 : for\ 0 \leq 4x^2 + y^2 \leq 1\}$. *We need to choose a normal cross-section to the circular orbits whose tangent field must satisfy* $\mathbf{w} = x\partial_x + y\partial_y$ *which produces curves of the form* (x_0e^t, y_0e^t)*; half lines emanating from the origin. Instead of using exponentials we take the normal cross-section to be* $C(r) = (0, r, r^2)$ *for* $0 \leq r \leq 1$.

The arc-length weight of the ruling orbits in S_1 *have weight* $\ell(\mathcal{O}_r) = 2\pi r$ *for* $0 \leq r \leq 1$ *and the weight of the entire surface is just the area beneath the curve which is* π. *Then formula* (3.12) *says that,*

$$\iint_S dx\ dy = \int_C \ell(\mathcal{O}_r)|\omega| = \int_{r=0}^{1}\int_{\theta=0}^{2\pi} r\ d\theta\ dr.$$

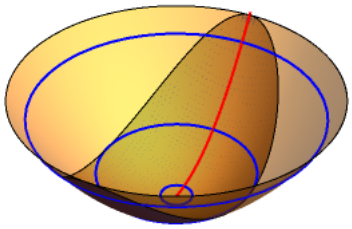

Figure 3.4: The two paraboloids are superimposed while some of the ruling orbits are traced in blue and our chosen normal cross-section in red.

This is exactly the change of variables from cartesian to polar coordinates. The weight for each ruling orbit in S_2 is

$$\ell(\mathcal{O}_r) = \begin{cases} 2\pi r & \text{if } 0 \leq r \leq 1/2 \\ 4\displaystyle\int_0^{\sqrt{\frac{1-r^2}{3}}} \sqrt{1 + \frac{x^2}{r^2 - x^2}}\, dx & \text{if } 1/2 \leq r \leq 1 \end{cases}$$

while the entire signature's weight is $\frac{\pi}{2}$.

In order to utilize the coarea formula (3.12), we need to have a normal cross-section to the ruling orbits foliating the surface. To this end we outline a systematic approach deriving $\mathbf{v}$, the infinitesimal generator to the ruling orbits. The main idea of the approach is to simplify the equations for the generating differential invariants κ and τ on $J^n(\mathbb{R}^3, 1)$ by (1) using the fact that $\mathbf{v}$ is in the Lie algebra and (2) by assuming that the ruling orbit used in the computation is in "normal form", [61]. The skeleton of the algorithm is as follows.

1. Pick any point p on the signature curve to a given rank 1 surface and consider its pre-image $\{\exp(t\mathbf{v})\cdot q\}$, which we will assume is one connected ruling orbit in S.

2. Evaluate κ and τ on the orbit $\{\exp(t\mathbf{v})\cdot q\}$ producing constant values $\kappa|_q$ and $\tau|_q$.

3. Mimic the algorithm in [57] to obtain simplified expressions for κ and τ to a $1-$parameter orbit in normal form at an appropriate base point z_0 (preferably the origin) in terms of the constants a_i from the linear combination of infinitesimal generators; $\widehat{\mathbf{v}} = \sum_1^r a_i\mathbf{v}_i$. Denote these expressions by $\kappa(a_i)$ and $\tau(a_i)$.

4. Solve the system of linear equations $\kappa(a_i) = \kappa|_q$ and $\tau(a_i) = \tau|_q$ for the constants.

5. Once the tangent vector field $\widehat{\mathbf{v}}$ to orbits in normal form is established, we use the fact that $\widehat{\mathbf{v}}$ is related to $\mathbf{v}$ by the adjoint.

First the moving frame machinery is used to find the differential invariants on $J^n(\mathbb{R}^3,1)$ and $J^n(\mathbb{R}^3,2)$ and the corresponding signature maps, respectively denoted by χ_1 and χ_2. The signature invariants on $J^n(\mathbb{R}^3,1)$ will be used throughout the process while those on $J^n(\mathbb{R}^3,2)$ are just used to pick out a particular ruling orbit $\{\exp(t\mathbf{v})\cdot q\}$, on the surface as step one above indicates.

In step two we evaluate the $J^n(\mathbb{R}^3,1)$ invariants κ and τ on the chosen ruling orbit $\{\exp(t\mathbf{v})\cdot q\}$ and denote those values by $\kappa|_q$ and $\tau|_q$. Note that these values should be constant, i.e., $\kappa_s|_q = \tau_s|_q = 0$.

In step three we use the algorithm in [57] to simplify the explicit formulas for κ and τ. The first step in simplifying the formulas results from assuming that the invariants will be evaluated on a generic $1-$parameter orbit $\mathcal{O}$ with infinitesimal generator $\widehat{\mathbf{v}} = \sum_1^r a_i\mathbf{v}_i$, for $\mathbf{v}_i \in \mathfrak{g}$. This is achieved by replacing the jets in the formulas with modified jets that are just rewritten in terms of $\widehat{\mathbf{v}}$. At this point the formulas will not seem especially simplified, in fact they may look worse. The modified jet coordinates can be further simplified by assuming that the orbit $\mathcal{O}$ is in *normal form* at some base point $\widehat{z}_0$, meaning that the orbit's $n-$jet at $\widehat{z}_0$ coincides with the fixed cross-section K used in the moving

frames construction: $j_n\mathcal{O}\big|_{\widehat{z}_0} \in K$. Thus, normal form imposes the evaluation of the modified jet coordinates at $\widehat{z}_0$ and setting those jets used in the cross-section equal to the appropriate constants specified by K. Then the jets in the explicit formulas for κ and τ are replaced by these further modified jets producing expressions involving the constants in the linear combination of $\widehat{\mathbf{v}}$, and we denote these simplified expressions by $\kappa(a_i)$ and $\tau(a_i)$.

Finally we solve the system: $\kappa(a_i) = \kappa|_q, \tau(a_i) = \tau|_q$, in terms of one of the constants to obtain $\widehat{\mathbf{v}}$. In reality the ruling orbits are likely not in normal form, but its infinitesimal generator $\mathbf{v}$ is related to $\widehat{\mathbf{v}}$ by the adjoint action; $\mathbf{v} = \mathrm{Ad}(\widehat{\mathbf{v}})$, that sends the base point $\widehat{z}_0$ lying on the orbit in normal form to any chosen base point z_0 on an appropriate orbit on the surface. Recall that the right moving frame outputs the group element that moves a point to the cross-section K, therefore the left moving frame does the opposite.

Example 15. *Consider the group action in equation* (2.7). *We are interested in simplifying the expressions for the invariants* $\kappa = \dfrac{y_{xx}}{(1+y_x^2)^{3/2}}$ *and* $\tau = \dfrac{u_x}{\sqrt{1+y_x^2}}$, *given that they are evaluated on an embedded curve,* $c(x) = (x, y(x), u(x))$, *that is known to be a* $1-$*parameter orbit,* $\mathcal{O}$ *induced by the generic infinitesimal generator* $\widehat{\mathbf{v}}$, *whose third prolongation is below.*

$$\begin{aligned}
\widehat{\mathbf{v}}^{(3)} &= \sum_{i=1}^{4} a_i \mathbf{v}_i^{(3)} \\
&= (a_1 + a_4 y)\partial_x + (a_2 - a_4 x)\partial_y + a_3\partial_u + a_4\Big((-1-y_x)\partial_{y_x} - y_x u_x \partial_{u_x}\Big) \\
&\quad - 3a_4 y_x y_{xx}\partial_{y_{xx}} - a_4(2y_x u_{xx} + u_x y_{xx})\partial_{u_{xx}} \\
&\quad - a_4(3y_{xx}^2 + 4y_x y_{xxx})\partial_{y_{xxx}} - a_4(3y_{xx}u_{xx} + 3y_x u_{xxx} + u_x y_{xxx})\partial_{u_{xxx}}.
\end{aligned}$$

The total derivative operator, $D_x = \dfrac{\partial}{\partial x} + \dfrac{dy}{dx}\dfrac{\partial}{\partial y} + \dfrac{du}{dx}\dfrac{\partial}{\partial u}$, *can also be tailored to this situation by evaluating the coefficients on a generic orbit resulting in the modified operator,*

$$\widehat{D}_x = \frac{\partial}{\partial x} + \Big(\frac{a_2 - a_4 x}{a_1 + a_4 y}\Big)\frac{\partial}{\partial y} + \Big(\frac{a_3}{a_1 + a_4 y}\Big)\frac{\partial}{\partial u}.$$

The values of the jets are obtained by applying the modified derivative operator $\widehat{D}_x$ *to the dependent variables* y *and* u *and their higher order derivatives. For this we introduce new notation* ψ^y_k *and* ψ^u_k *defined below to escape from writing unwieldily expressions in equations* (3.13), (3.14).

$$y_k(x,y,u) = \psi^y_k(x,y,u) = \widehat{D}^k_x(y) = \widehat{D}_x(\psi^y_{k-1}(x,y,u)),$$
$$u_k(x,y,u) = \psi^u_k(x,y,u) = \widehat{D}^k_x(u) = \widehat{D}_x(\psi^u_{k-1}(x,y,u)).$$

Using the notation above, the jets can be expressed as,

$$\begin{aligned}
y_x &= \psi^y_1(x,y,u) = \frac{a_2 - a_4 x}{a_1 + a_4 y},\\
u_x &= \psi^u_1(x,y,u) = \frac{a_3}{a_1 + a_4 y},\\
y_{xx} &= \psi^y_2(x,y,u) = \frac{-a_4}{a_1 + a_4 y} - \frac{a_4(a_2 - a_4 x)^2}{(a_1 + a_4 y)^3},\\
u_{xx} &= \psi^u_2(x,y,u) = -\frac{a_3 a_4 (a_2 - a_4 x)}{(a_1 + a_4 y)^3},\\
y_{xxx} &= \psi^y_3(x,y,u) = \frac{2a_4^2(a_2 - a_4 x)}{(a_1 + a_4 y)^3} + \Big(\frac{a_2 - a_4 x}{a_1 + a_4 y}\Big)\left(\frac{a_4^2}{(a_1 + a_4 y)^2} + \frac{3a_4^2(a_2 - a_4 x)^2}{(a_1 + a_4 y)^4}\right).
\end{aligned}$$

The restriction of the signature map to $\mathcal{O}$ *is achieved by replacing* $y_k(x,y,u)$ *with* $\psi^y_k(x,y,u)$ *and* $u_k(x,y,u)$ *with* $\psi^u_k(x,y,u)$ *yielding,*

$$\tau = \frac{\psi^u_1}{\sqrt{1 + (\psi^y_1)^2}}, \qquad \kappa = \frac{\psi^y_2}{\sqrt{1 + (\psi^y_1)^2}}, \tag{3.13}$$

$$\tau_s = \frac{\psi^u_2}{1 + (\psi^y_1)^2} + \frac{\psi^u_1 \psi^y_1 \psi^y_2}{1 + (\psi^y_1)^2}, \qquad \kappa_s = \frac{\psi^y_3}{1 + (\psi^y_1)^2} - \frac{\psi^y_1 (\psi^y_2)^2}{(1 + (\psi^y_1)^2)^2}. \tag{3.14}$$

The expressions above are likely to be quite unwieldily in general, but there is hope for we can simplify them by applying a preliminary group transformation to place $\mathcal{O}$ *into "normal form" with respect to some point* $z_0 \in \mathcal{O}$*, meaning that at* $\mathcal{O}|_{z_0} \in K$*, where* K *is the cross-section used in the moving frame construction. In our case,* $K^1 = \{x = y = u = y_x = 0\}$*. This restricts the base point to be*

$z_0 = (0,0,0)$ and y_x forces the tangent line to $\mathcal{O}$ at z_0 to be horizontal; $\psi_1^y(z_0) = 0$, implying $a_2 = 0$. Then the jet coordinates become

$$\psi_1^u(z_0) = \frac{a_3}{a_1}, \quad \psi_2^y(z_0) = \frac{a_4}{a_1}, \quad \psi_2^u(z_0) = 0, \quad \psi_3^y(z_0) = 0.$$

Substitution of the above expressions into equations (3.13), *and* (3.14) *produces the simplified invariants,*

$$\tau = \frac{a_3}{a_1}, \qquad \kappa = \frac{a_4}{a_1}, \qquad \kappa_s = 0, \qquad \tau_s = 0. \tag{3.15}$$

Note that these expressions nicely illustrate the essence of theorem 11.

There are three types of rank 1 surfaces under this action corresponding to the three $1-$parameter orbits; circles associated to the generator $\mathbf{v_4} = y\partial_x - x\partial_y$, lines generated by a linear combination of $\mathbf{v_1} = \partial_x, \mathbf{v_2} = \partial_y$, and $\mathbf{v_3} = \partial_u$, and helices generated by $\mathbf{v_3}$ and $\mathbf{v_4}$.

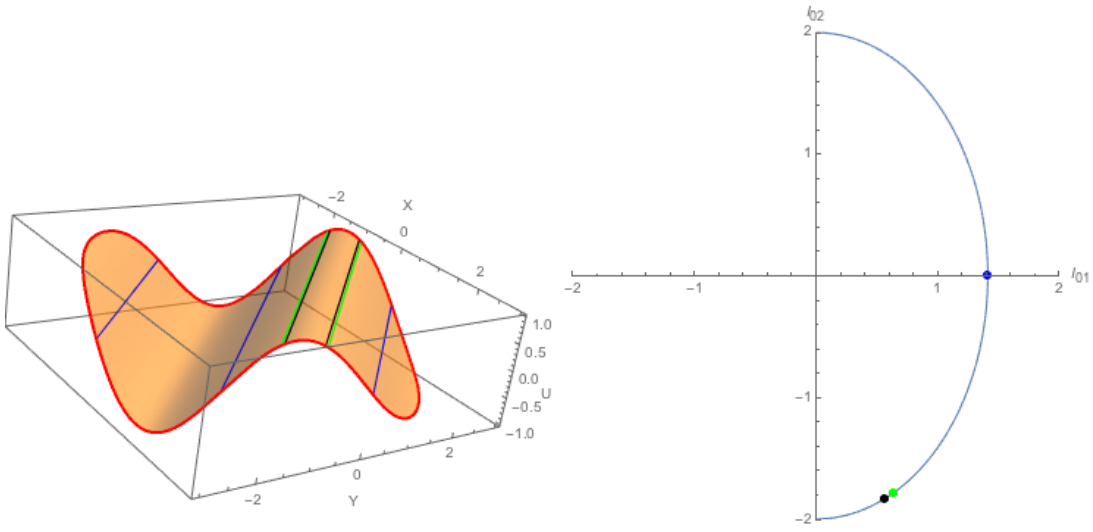

Figure 3.5: Left: Rank 1 surface $\sin(x+y)$ with several ruling orbits outlined. Right: Signature of surface and ruling orbits.

We are interested in finding the infinitesimal generator to the ruling orbits of the surface $u(x,y) = \sin(\alpha x + \beta y)$, using the algorithm outlined earlier. By

choosing a particular point on the surface's signature and considering the pre-image, we can pick out an individual ruling orbit, say $\mathcal{O}$ *and compute* $\kappa|_{\mathcal{O}}$ *and* $\tau|_{\mathcal{O}}$ *to determine the type of orbits that foliate* S*. In this case we find that* $\kappa = \tau = 0$ *implying the orbits are lines. Therefore it must be that* $a_3 = a_4 = 0$ *and so* $\widehat{\mathbf{v}} = a_1\mathbf{v_1}$*. Next, we pick a base point* $z_0 = (x_0, y_0, u(x_0, y_0)) \in \mathcal{O} \subset S$ *and compute the left moving frame at this point, since it is the left moving frame that outputs the group element that would take the base point off of the cross-section and map it to* z_0*. The right moving frame is given in equation* (2.9) *and the left moving frame is the inverse of the right, so* $\mathbf{v} = \rho(z_0)^{-1} \cdot \widehat{\mathbf{v}} \cdot \rho(z_0)$ *for the right moving frame* ρ*. We take* $z_0 = (0, 0, 0)$ *then,* $\rho(0, 0, 0) = (a, b, c, \theta) = (0, 0, 0, -\tan^{-1}(-\alpha/\beta))$*. Then the vector field to the ruling orbit through* z_0 *is given by the following.*

$$
\begin{aligned}
\mathbf{v} &= \rho(z_0)^{-1}\widehat{\mathbf{v}}\rho(z_0) \\
&= \begin{bmatrix} \frac{\beta}{\sqrt{\alpha^2+\beta^2}} & \frac{\alpha}{\sqrt{\alpha^2+\beta^2}} & 0 & 0 \\ -\frac{\alpha}{\sqrt{\alpha^2+\beta^2}} & \frac{\beta}{\sqrt{\alpha^2+\beta^2}} & 0 & 0 \\ 0 & 0 & 1 & 0 \\ 0 & 0 & 0 & 1 \end{bmatrix} \begin{bmatrix} 0 & 0 & 0 & a_1 \\ 0 & 0 & 0 & 0 \\ 0 & 0 & 0 & 0 \\ 0 & 0 & 0 & 0 \end{bmatrix} \begin{bmatrix} \frac{\beta}{\sqrt{\alpha^2+\beta^2}} & -\frac{\alpha}{\sqrt{\alpha^2+\beta^2}} & 0 & 0 \\ \frac{\alpha}{\sqrt{\alpha^2+\beta^2}} & \frac{\beta}{\sqrt{\alpha^2+\beta^2}} & 0 & 0 \\ 0 & 0 & 1 & 0 \\ 0 & 0 & 0 & 1 \end{bmatrix} \\
&= \frac{a_1}{\sqrt{\alpha^2+\beta^2}} \begin{bmatrix} 0 & 0 & 0 & \beta \\ 0 & 0 & 0 & -\alpha \\ 0 & 0 & 0 & 0 \\ 0 & 0 & 0 & 0 \end{bmatrix}.
\end{aligned}
$$

We obtain a constant multiple of the vector fields $\mathbf{v} = \beta\partial_x - \alpha\partial_y$*, which is exactly what we are looking for.*

For a more involved example consider the rank 1 surface foliated by circles; $u(x, y) = \sin((x-1)^2 + y^2)$*. This will be established by picking out a single ruling orbit and evaluating* κ *and* τ *there. Suppose we pick the circle of radius 1 so that* $\kappa = 1$ *and* $\tau = 0$ *implying that* $a_3 = 0$ *and* $a_1 = a_4$*. We take* $a_1 = 1$ *so that the vector field to the circle of radius 1 in normal form is* $\widehat{\mathbf{v}} = (-y+1)\partial_x + x\partial_y$*. To*

figure out $\mathbf{v}$ *we compute the group elements that send the point* $(0, 0, \sin(1))$ *on normal form unit circle to some chosen base point on the ruling orbit with* $\kappa = 1$ *lying on the surface. We choose the base point* $z_0 = \left(1 + \frac{\sqrt{2}}{2}, \frac{\sqrt{2}}{2}, \sin(1)\right)$ *where the tangent line has slope* -1*. Then,*

$$
\begin{aligned}
&\mathbf{v} = \rho(z_0)^{-1}\widehat{\mathbf{v}}\rho(z_0) \\
&= \begin{bmatrix} \cos\frac{\pi}{4} & -\sin\frac{\pi}{4} & 0 & -\frac{\sqrt{2}}{2} \\ \sin\frac{\pi}{4} & \cos\frac{\pi}{4} & 0 & -1-\frac{\sqrt{2}}{2} \\ 0 & 0 & 1 & -\sin(1) \\ 0 & 0 & 0 & 1 \end{bmatrix}^{-1} \begin{bmatrix} 0 & -1 & 0 & -1 \\ 1 & 0 & 0 & 0 \\ 0 & 0 & 0 & 0 \\ 0 & 0 & 0 & 0 \end{bmatrix} \begin{bmatrix} \cos\frac{\pi}{4} & -\sin\frac{\pi}{4} & 0 & -\frac{\sqrt{2}}{2} \\ \sin\frac{\pi}{4} & \cos\frac{\pi}{4} & 0 & -1-\frac{\sqrt{2}}{2} \\ 0 & 0 & 1 & -\sin(1) \\ 0 & 0 & 0 & 1 \end{bmatrix} \\
&= \begin{bmatrix} 0 & -1 & 0 & 0 \\ 1 & 0 & 0 & -1 \\ 0 & 0 & 0 & 0 \\ 0 & 0 & 0 & 0 \end{bmatrix}.
\end{aligned}
$$

Thus $\mathbf{v} = -y\partial_x + (x-1)\partial_y$*, which is exactly the tangent vector field to circles centered at* $(1, 0)$ *shown in the figure below.*

The methods used to create fully regular signature congruent surfaces can also be employed to create ones with varying rank. Let $S = S_2 \cup S_n$ where S_2 has rank 2 and S_n is either of rank 0 or 1; $n = 0$ or $n = 1$. Then $\partial S = A \cup B$ for $A \subset \partial S_2$ and $B \subset \partial S_n$ (assume that if nonempty then they contain a connected 1-dimensional subset of the boundary). There are two characterizations of such a surface that we are interested in; either $B \neq \varnothing$ or $B = \varnothing$. If $B = \varnothing$, then the boundary of the surface ∂S, is only in contact with the rank 2 portion and in most cases, cannot be altered without disturbing the signature. For the same reason the boundary between S_2 and S_n that lies within the interior of S cannot be altered either. This makes it difficult to build a signature congruent family of surfaces with this boundary characteristic. On the other hand, if $B \neq \varnothing$, then B is more likely to have the potential to be smoothly deformed while leaving the

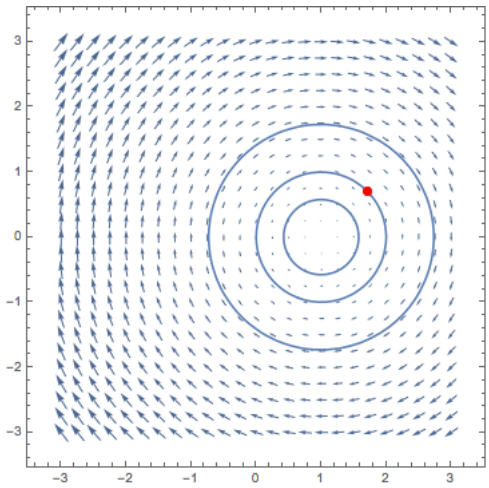

Figure 3.6: Rotational vector field for circles with center (1,0) and three such circles. The red dot is the point z_0 projected to the $xy-$plane.

surface's signature manifold intact, though the weighted signature may or may not change.

Chapter 4

Discrete Signatures

In this chapter, we consider the consequences of approximating submanifolds by points and methodologies that may prove computationally beneficial. In our computational examples we incorporated a finite difference approach by approximating the derivatives in the signature invariants using second order centered finite difference equations. Though we do not address the accuracy of this numerical method, more on this front can be found in [1, 2, 20].

Due to the likely high order of the signature invariants, the discrete signature could benefit from the use of group invariant numerical approximations, though each action would require its own scheme. In [7, 13], an explicit Euclidean-invariant numerical scheme, based on suitable combinations of Euclidean joint invariants based on the mesh points used to approximate a planar curve was developed for the purposes of approximating the Euclidean curvature. In general, any $G-$invariant numerical approximation to a differential invariant must be governed by a function of the joint invariants of G, [55]. For instance, any Euclidean invariant approximation to the Euclidean curvature of a plane curve must be based on Euclidean distances between the mesh points. Naturally, error analysis of these schemes should be practiced to assess their accuracy and stability.

Special discretization methods may also result in more accurate and stable discrete signatures. For curves, an ordered set of sample points gives rise to an

ordered bivertex decomposition that provides more geometrical information; see example 16.

For actions admitting a minimal moving frame, one can sample a curve in such a way that $\Delta = \int_{c(t_i)}^{c(t_{i+1})} ds$, for all adjacent sample points $c(t_i)$ and $c(t_{i+1})$, and for some small spacing constant $\Delta > 0$. We call such a discretization a *uniform (equally spaced) invariant discretization*, which is the discrete analogue of a unit-speed parametrization. Any numerical method using this natural parameter to compute the discrete signature is invariant. Moreover, the computation for the $ds-$weight of $\Gamma \subset \Sigma$ is greatly simplified to multiplication by the number of sample points in Γ by Δ, so that the weight is always proportional the number of sample points. Thus this discrete signature is a physical manifestation of the $ds-$weighted signature which can be analyzed at a glance, see example 17.

Similar methods could be employed for surfaces. Specifically, we could use knowledge of the infinitesimal generator to the ruling orbits of a rank 1 surface to tailor our sampling methods so that it better outlines the ruling orbits. Adaptable meshes that increase in fineness where derivatives take on larger values would aid in obtaining more accurate discrete signatures and weight computations.

Lastly, though totally singular submanifolds have no signature, the fact that the submanifold is sampled indicates its existence. Now, depending on the discretization method, we may be able to say more given the number of sample points.

Example 16. *Return to example 10, and divide the parameter's interval into equal subintervals of length* $\Delta t = .01$ *obtaining the point set* $\{x(t_i), u(t_i)\} = \{x_i, u_i\}$. *Each parametric curve in the family is defined on the same interval resulting in the same number of sample points, in this case 3244, of which approximately 61% lie on straight line segments for each of the four curves presented in figure 3.2. The table below lists the number of sample points on the line segments starting at the origin and moving counterclockwise about the curve.*
The arc-length weight of an individual line segment S is approximated via

a	b	c	d
98	298	498	998
898	700	500	0
100	300	498	1000
899	700	500	0

Table 4.1: The headings refer to the curves in figure 3.2 and the numbers from top to bottom are the number of sample points that lie on straight line segments of the rectangular curves as you move counterclockwise starting at the origin.

$$\nu(\chi(S)) \approx \sum_{(x_i,u_i)\in S} \sqrt{\dot{x}_i^2 + \dot{u}_i^2}\Delta t = \frac{1}{2} \sum_{(x_i,u_i)\in S} \sqrt{(x_{i+1} - x_{i-1})^2 + (u_{i+1} - u_{i-1})^2}.$$

Along corresponding line segments $\sqrt{\dot{x}_i^2 + \dot{u}_i^2}$ *takes the same constant value for each of the curves, so the weight is proportional to the number of points. Table 4.1 shows the weight of individual line segments clearly illustrating that the curves are inequivalent.*

Example 17. *The SO(2) signature is parametrized by the radius* r *and its invariant derivative* r_s *which is the change in the radius as a function of the angle* θ*. Therefore we require the curve be locally expressible in polar coordinates. Uniform invariant discretization* $\{(\theta_i, r(\theta_i)\}$ *requires that the sample points be chosen so that* $r(\theta_{i+1}) = r(\theta_i + \Delta\theta)$ *for some constant* $\Delta\theta > 0$ *since the unique lowest order* $1-$*form is* $ds = d\theta$*.*

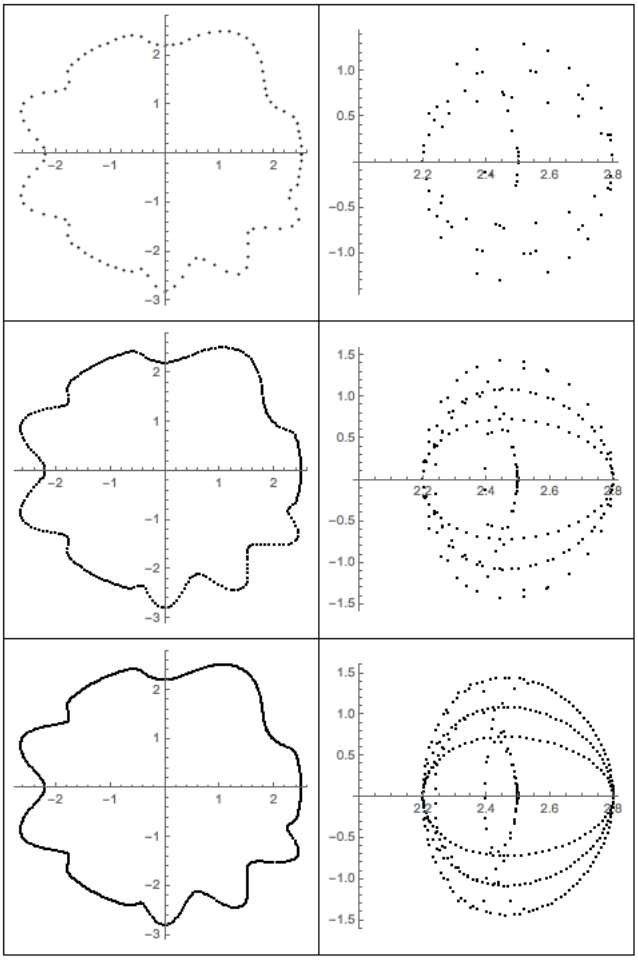

Figure 4.1: Left: Cogwheel with uniform invariant discretization $\Delta\theta = .06, .02, .01$ from top to bottom. Right: Discrete SO(2) signature computed from corresponding discrete cogwheel.

Chapter 5

Conclusion and Discussion

To summarize, weighted signatures provide more geometrical information from measuring intrinsic invariant quantities of the underlying submanifold. This extra information does help differentiate between some, but not all, pairs of signature congruent submanifolds. Specifically, weighted signatures have trouble with signature congruent curves that are assembled with the same rank 1 pieces and signature congruent surfaces that vary in shape, that is, their boundaries are not equivalent. In the latter case, the signature of the boundary is a viable solution, but occlusions could hamper its effectiveness. In the former case, an ordered bivertex decomposition will solve the issue, though this requires that the decomposition be obtained from identically oriented curves. For instance, in example 11, the ordered bivertex decomposition of the Euclidean inequivalent cogwheels would be identical if the orientation for one cogwheel was taken to be counterclockwise while the other was clockwise. Moreover, the more flexible notion of the index, that alone can determine inequivalence, is encoded in the ordered bivertex decomposition or the weight.

Though we have spoken about "the" weighted signature throughout, there is flexibility in the choice of weight which may prove useful in other ways. For example, the analysis of an image to diagnose breast tumors as benign or malignant may decrease the necessity of invasive procedures such as biopsies as well as offer

other benefits. In [33], the Euclidean signature curve of $2-$dimensional projections of 78 malignant and 78 benign tumors were investigated. It was determined that the range for κ_s was larger for malignant tumors. This is due to the difference in growth rates of the two types of tumors which cause finger-like proliferations on the surface of malignant tumors called spiculation, as opposed to the more regular smooth surface of a benign tumor. Thus the weighted signature with density $\omega = |\kappa_s|\ ds$ will emphasize the presence of spiculation and aid in cancer classification. An interesting project would be to replicate this type of research using weighted signatures and if possible weighted signatures of the surface of tumors.

The discussion above about applications to tumor diagnosis, sparks the need for a meaningful representation of a weighted signature, whether it be tabular, graphical, or something else, especially in the cases when the signature lives in $\mathbb{R}^m$ for $m > 3$. For instance, the signature of a surface and the signature of its $1-$dimensional boundary, live in different jet spaces. The development of a space that houses both signatures simultaneously may prove beneficial.

More information about orbits in rank varying submanifolds can be gathered from the invariants with respect to a smaller subgroup $H \subset G$. The inductive moving frame method outlines how to construct a moving frame for the larger group G and express $G-$invariants in terms of their H counterparts, [42, 43, 60]. But an $H-$invariant isn't necessarily a $G-$invariant, implying that those orbits induced by elements in the Lie algebra of G, but not H, will be rank 1 with respect to the $H-$signature, Σ_H. It also means that discrepancies in Σ_H could manifest from $G-$transformations that are not $H-$transformations, which may be avoided by performing the appropriate transformation to the submanifold beforehand. For example, let $G = \mathrm{E}(2)$ and $H = \mathrm{SO}(2)$. The orbits for the Euclidean action are lines and circles, but only circles centered at the origin constitute $1-$parameter orbits for the action of rotation about the origin. Thus, Euclidean signature congruent curves may have different SO(2) signatures manifolds. But before the SO(2) signature can be determined, the curves should be translated so that their center of mass is at the origin to eliminate any discrepancies due to translations.

Example 18. *The following four simple closed planar curves are the same appearing in the motivation section on weighted signatures, except that each curve has been translated so that its center of mass is located at the origin. In effect, eliminating any translations that would effect the SO(2) signature. It is obvious from the SO(2) signature in figure 5.1, that the four curves are rotationally inequivalent and therefore they are also inequivalent with respect to the Euclidean action.*

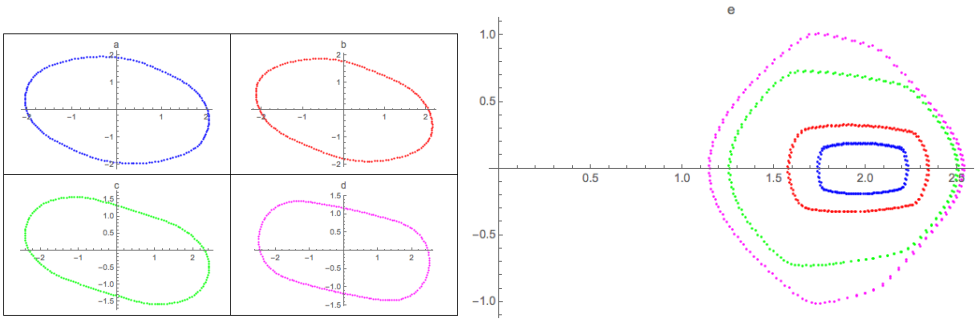

Figure 5.1: Top: Translated curves so that center of mass is located at the origin. Bottom: Discrete SO(2) signature of the curves above. The horizontal axis represents the radius while the vertical axis is the change in the radius with respect to SO(2) arc-length which can be thought of as the change in the radius with respect to the change in the angle.

Of course, the discussion of applications is of little consequence if implementation is too computationally expensive or inaccurate. Thus, investigation into methods from numerically invariant computations to the software doing the analysis is needed to bring all the pieces together and further the attractiveness of signatures to real world applications. In doing so it is natural to develop a meaningful metric, measuring the distance between weighted signatures. This may be split into two; measuring the Euclidean distance between signature manifolds or discrete signatures and developing a metric on the weight of certain subsets. Not only is this essential for determining accuracy and closeness, it is also an important component in an autonomous shape recognition scheme.

References

[1] Aghayan, R., Ellis, T., and Dehmeshki, J. Joint invariants in signature theory applied to object recognition. In *Proceedings of the International Conference on Image Processing, Computer Vision, and Pattern Recognition (IPCV)* (2012), The Steering Committee of The World Congress in Computer Science, Computer Engineering and Applied Computing (WorldComp), p. 1.

[2] Aghayan, R., Ellis, T., and Dehmeshki, J. Planar numerical signature theory applied to object recognition. *J. Math. Imaging Vision 48*, 3 (2014), 583–605.

[3] Akivis, M. A., and Rosenfeld, B. A. *Élie Cartan (1869–1951)*, vol. 123 of *Translations of Mathematical Monographs*. American Mathematical Society, Providence, RI, 1993. Translated from the Russian manuscript by V. V. Goldberg.

[4] Anderson, I. M. The variational bicomplex. Tech. rep., Utah State Technical Report, 1989, http://math. usu. edu/ fg mp, 1989.

[5] Bachman, D. *A geometric approach to differential forms*. Springer Science & Business Media, 2012.

[6] Bobenko, A. I., Sullivan, J. M., Schröder, P., and Ziegler, G. *Discrete differential geometry*. Springer, 2008.

[7] Boutin, M. Numerically invariant signature curves. *International Journal of Computer Vision 40*, 3 (2000), 235–248.

[8] Boutin, M. Polygon recognition and symmetry detection. *Foundations of Computational Mathematics 3*, 3 (2003), 227–271.

[9] Boutin, M. Polygon recognition and symmetry detection. *Found. Comput. Math. 3*, 3 (2003), 227–271.

[10] Brown, R. From groups to groupoids: a brief survey. *Bull. London Math. Soc. 19*, 2 (1987), 113–134.

[11] Bruckstein, A. M., Holt, R. J., Netravali, N., and Richardson, T. J. Invariant signatures for planar shape recognition under partial occlusion. In *Pattern Recognition, 1992. Vol. I. Conference A: Computer Vision and Applications, Proceedings., 11th IAPR International Conference on* (1992), IEEE, pp. 108–112.

[12] Bruckstein, A. M., and Shaked, D. Skew symmetry detection via invariant signatures. In *Computer Analysis of Images and Patterns* (1995), Springer, pp. 17–24.

[13] Calabi, E., Olver, P. J., Shakiban, C., Tannenbaum, A., and Haker, S. Differential and numerically invariant signature curves applied to object recognition. *International Journal of Computer Vision 26*, 2 (1998), 107–135.

[14] Cartan, É. *La structure des groupes de transformations continus et la théorie du trièdre mobile.* 1910.

[15] Cartan, E. La méthode du repére mobile, la théorie des groupes continues, et les espaces généralisés exposés de géométrie no. 5. *Hermann, Paris* (1935).

[16] Cartan, E. *La théorie des groupes finis et continus et la géométrie différentielle: traitées par la méthode du repère mobile.* Gauthier-Villars, 1937.

[17] Chern, S. S. Moving frames. *Astérisque*, Numero Hors Serie (1985), 67–77. The mathematical heritage of Élie Cartan (Lyon, 1984).

[18] Crainic, M., and Fernandes, R. L. Lectures on integrability of Lie brackets. In *Lectures on Poisson geometry*, vol. 17 of *Geom. Topol. Monogr.* Geom. Topol. Publ., Coventry, 2011, pp. 1–107.

[19] Crevier, D. *AI: The tumultuous history of the search for artificial intelligence*. Basic Books, Inc., 1993.

[20] Dalle, D. Comparison of numerical techniques for euclidean curvature. *Rose–Hulman Undergraduate Math. J 7*, 1 (2006), 1–29.

[21] Do Carmo, M. P. *Differential forms and applications*. Springer Science & Business Media, 2012.

[22] Do Carmo, M. P., and Do Carmo, M. P. *Differential geometry of curves and surfaces*, vol. 2. Prentice-hall Englewood Cliffs, 1976.

[23] Eisenhart, L. P. *A treatise on the differential geometry of curves and surfaces*. Dover Publications, Inc., New York, 1960.

[24] Faugeras, O. *Cartan's moving frame method and its application to the geometry and evolution of curves in the euclidean, affine and projective planes*. Springer, 1994.

[25] Fels, M., and Olver, P. J. Moving coframes: 1. a practical algorithm. *Acta Applicandae Mathematica 51*, 2 (1998), 161–213.

[26] Fels, M., and Olver, P. J. Moving coframes: 2. regularization and theoretical foundations. *Acta Applicandae Mathematica 55*, 2 (1999), 127–208.

[27] Fels, M. E. *Some applications of Cartan's method of equivalence to the geometric study of ordinary and partial differential equations*. ProQuest LLC, Ann Arbor, MI, 1993. Thesis (Ph.D.)–McGill University (Canada).

[28] Gardner, R. B. *The method of equivalence and its applications.* SIAM, 1989.

[29] Gray, A., Abbena, E., and Salamon, S. *Modern differential geometry of curves and surfaces with Mathematica®*, third ed. Studies in Advanced Mathematics. Chapman & Hall/CRC, Boca Raton, FL, 2006.

[30] Green, M. L. The moving frame, differential invariants and rigidity theorems for curves in homogeneous spaces. *Duke Math. J. 45*, 4 (1978), 735–779.

[31] Griffiths, P. On Cartan's method of Lie groups and moving frames as applied to uniqueness and existence questions in differential geometry. *Duke Math. J. 41* (1974), 775–814.

[32] Grim, A., O?Connor, T., Olver, P. J., Shakiban, C., Slechta, R., and Thompson, R. Automatic reassembly of three-dimensional jigsaw puzzles. *International Journal of Image and Graphics 16*, 02 (2016), 1650009.

[33] Grim, A. M., and Shakiban, C. Applications of signatures in diagnosing breast cancer. *Minnesota Journal of Undergraduate Mathematics 1*, 1 (2015).

[34] Guggenheimer, H. W. *Differential geometry.* Dover Publications, Inc., New York, 1977. Corrected reprint of the 1963 edition, Dover Books on Advanced Mathematics.

[35] Hickman, M. S. Euclidean signature curves. *Journal of Mathematical Imaging and Vision 43*, 3 (2012), 206–213.

[36] Hoff, D. J., and Olver, P. J. Extensions of invariant signatures for object recognition. *Journal of mathematical imaging and vision 45*, 2 (2013), 176–185.

[37] Hoff, D. J., and Olver, P. J. Automatic solution of jigsaw puzzles. *Journal of mathematical imaging and vision 49*, 1 (2014), 234–250.

[38] Hubert, E. Generation properties of maurer-cartan invariants, http://hal.inria.fr/inria-00194528.

[39] Hubert, E. Differential invariants of a lie group action: syzygies on a generating set. *Journal of Symbolic Computation 44*, 4 (2009), 382–416.

[40] Hubert, E. Algebraic and differential invariants. *Foundations of computational mathematics, Budapest*, 403 (2011).

[41] Kamran, N. Contributions to the study of the equivalence problem of Élie Cartan and its applications to partial and ordinary differential equations. *Acad. Roy. Belg. Cl. Sci. Mém. Collect. 8º (2) 45*, 7 (1989), 122.

[42] Kogan, I. A. *Inductive approach to Cartan's moving frame method with applications to classical invariant theory*. ProQuest LLC, Ann Arbor, MI, 2000. Thesis (Ph.D.)–University of Minnesota.

[43] Kogan, I. A. Inductive construction of moving frames. *Contemporary Mathematics 285* (2001), 157–170.

[44] Kogan, I. A., and Olver, P. J. The invariant variational bicomplex. *Contemporary Mathematics 285* (2001), 131–144.

[45] Lamdan, Y., Schwartz, J. T., and Wolfson, H. J. Affine invariant model-based object recognition. *Robotics and Automation, IEEE Transactions on 6*, 5 (1990), 578–589.

[46] Luo, C., Ge, X., and Wang, Y. Uniformization and density adaptation for point cloud data via graph laplacian. Tech. rep., Tech report OSU-CISRC-11/14-TR19, Ohio State University, 2014.

[47] Mansfield, E. L. *A practical guide to the invariant calculus*, vol. 26. Cambridge University Press, 2010.

[48] Monterde, J. Salkowski curves revisited: A family of curves with constant curvature and non-constant torsion. *Computer Aided Geometric Design 26*, 3 (2009), 271–278.

[49] Musso, E., and Nicolodi, L. Invariant signatures of closed planar curves. *Journal of Mathematical Imaging and Vision 35*, 1 (2009), 68–85.

[50] Olver, P. J. *Equivalence, invariants, and symmetry*. Cambridge University Press, Cambridge, 1995.

[51] Olver, P. J. Pseudo-stabilization of prolonged group actions i. the order zero case. *Journal of Nonlinear Mathematical Physics 4*, 3-4 (1997), 271–277.

[52] Olver, P. J. *Classical invariant theory*, vol. 44. Cambridge University Press, 1999.

[53] Olver, P. J. *Applications of Lie groups to differential equations*, vol. 107. Springer Science & Business Media, 2000.

[54] Olver, P. J. Moving frames and singularities of prolonged group actions. *Selecta Mathematica 6*, 1 (2000), 41–77.

[55] Olver, P. J. Joint invariant signatures. *Foundations of computational mathematics 1*, 1 (2001), 3–68.

[56] Olver, P. J. Generating differential invariants. *Journal of Mathematical Analysis and Applications 333*, 1 (2007), 450–471.

[57] Olver, P. J. Differential invariants of maximally symmetric submanifolds. *J. Lie Theory 19*, 1 (2009), 79–99.

[58] Olver, P. J. Moving frames and differential invariants in centro-affine geometry. *Lobachevskii Journal of Mathematics 31*, 2 (2010), 77–89.

[59] Olver, P. J. Differential invariant algebras. In *Symmetries and related topics in differential and difference equations*, vol. 549 of *Contemp. Math.* Amer. Math. Soc., Providence, RI, 2011, pp. 95–121.

[60] Olver, P. J. Recursive moving frames. *Results in Mathematics 60*, 1-4 (2011), 423–452.

[61] Olver, P. J. Normal forms for submanifolds under group actions. *preprint, University of Minnesota* (2013).

[62] Olver, P. J. The symmetry groupoid and weighted signature of a geometric object. *J. Lie Theory 26*, 1 (2016), 235–267.

[63] Ondich, J. A differential constraints approach to partial invariance. *European J. Appl. Math. 6*, 6 (1995), 631–637.

[64] O'Neill, B. *Elementary differential geometry.* Academic Press, New York-London, 1966.

[65] Ovsiannikov, L. V. *Group analysis of differential equations.* Academic Press, Inc. [Harcourt Brace Jovanovich, Publishers], New York-London, 1982. Translated from the Russian by Y. Chapovsky, Translation edited by William F. Ames.

[66] Ovsienko, V., and Tabachnikov, S. *Projective differential geometry old and new*, vol. 165 of *Cambridge Tracts in Mathematics.* Cambridge University Press, Cambridge, 2005. From the Schwarzian derivative to the cohomology of diffeomorphism groups.

[67] Sapiro, G. *Geometric partial differential equations and image analysis.* Cambridge University Press, Cambridge, 2001.

[68] Singer, I. M., and Sternberg, S. The infinite groups of lie and cartan part i,(the transitive groups). *Journal d'analyse mathématique 15*, 1 (1965), 1–114.

[69] Szeliski, R. *Computer vision: algorithms and applications*. Springer Science & Business Media, 2010.

[70] Tresse, A. Sur les invariants différentiels des groupes continus de transformations. *Acta mathematica 18*, 1 (1894), 1–88.

[71] Weinstein, A. Groupoids: unifying internal and external symmetry. A tour through some examples. *Notices Amer. Math. Soc. 43*, 7 (1996), 744–752.

[72] Winger, R. M. *An introduction to projective geometry*. Dover Publications, Inc., New York, 1962.

[73] Wu, S., Li, Y., and Zhang, J. A viewpoint invariant signature descriptor for curved shape recognition. In *Robotics and Biomimetics, 2007. ROBIO 2007. IEEE International Conference on* (2007), IEEE, pp. 1121–1126.

[74] Yano, K., and Ishihara, S. *Tangent and cotangent bundles: differential geometry*, vol. 16. Dekker, 1973.